

Capacity of Distributed Storage Systems with Clusters and Separate Nodes

Jingzhao Wang, Tinghan Wang, Yuan Luo, *Member, IEEE*, and Kenneth W. Shum *Senior Member, IEEE*

Abstract—In distributed storage systems (DSSs), the optimal tradeoff between node storage and repair bandwidth is an important issue for designing distributed coding strategies to ensure large scale data reliability. The capacity of DSSs is obtained as a function of node storage and repair bandwidth parameters, characterizing the tradeoff. There are lots of works on DSSs with clusters (racks) where the repair bandwidths from intra-cluster and cross-cluster are differentiated. However, separate nodes are also prevalent in the realistic DSSs, but the works on DSSs with clusters and separate nodes (CSN-DSSs) are insufficient. In this paper, we formulate the capacity of CSN-DSSs with one separate node for the first time where the bandwidth to repair a separate node is of cross-cluster. Consequently, the optimal tradeoff between node storage and repair bandwidth are derived and compared with cluster DSSs. A regenerating code instance is constructed based on the tradeoff. Furthermore, the influence of adding a separate node is analyzed and formulated theoretically. We prove that when each cluster contains R nodes and any k nodes suffice to recover the original file (MDS property), adding an extra separate node will keep the capacity if $R|k$, and reduce the capacity otherwise.

I. INTRODUCTION

In the age of big data, massive amount of data are generated and stored in large data centers every day, where ensuring the data reliability is an important issue [16]. Erasure coding is widely used to tolerate node failures in distributed storage systems (DSSs) [2], [7], [17], [19], [37], where the original data are encoded and stored in multiple nodes. If a node failure happens, a newcomer is generated by downloading data from other nodes, which may incur high repair bandwidth [34]. The authors of [9] proposed regenerating codes to balance the node storage and repair bandwidth, which is characterized by the capacity of DSSs with homogeneous node parameters [11], meaning that all the storage nodes are undifferentiated.

On the other hand, in heterogeneous DSSs [11], [36], the storage and repair bandwidth parameters are different for different nodes based on the variety of real storage devices. In realistic storage systems, nodes are generally grouped with clusters (racks) [12], where the intra-cluster networks are often faster and cheaper. In order to make use of the communication resource efficiently, it is necessary to differentiate intra-cluster and cross-cluster bandwidths. Additionally, the cross-cluster bandwidth is often constrained in modern data centers [16]. For instance the available cross-cluster bandwidth for each

node is only $1/5$ to $1/20$ of the intra-cluster bandwidth in some cases [4], [8], [30]. It is efficient and practical to consider the balancing problem of the storage and repair bandwidth under realistic network topology. In [20], [32], the authors proposed tree-based topology-aware repair schemes considering networks with heterogeneous link capacities. In [26], Sipos *et al.* proposed a general network aware framework to reduce the repair bandwidth in heterogeneous and dynamic networks.

In [14], [15], [16], the authors investigated multi-cluster (rack) models to reduce the cross-cluster bandwidth, where data from nodes in each cluster were collected and transmitted with a relay node to repair a fail one. Coding strategies were proposed to minimize the cross-cluster repair bandwidth, which were deployed to verify the performance in hierarchical data centers in [14], [16]. In [1], [23], the authors also investigated cluster DSSs with relay nodes which were not only used for node repair, but also used for data collection. In [25], the authors proposed a data placement method to reduce the cross-cluster bandwidth on data reconstruction in the cluster DSS model without relay nodes. The DSS model with two clusters was considered in [6], [22]. In [27], the authors first proposed algorithms to characterize the capacity of the cluster DSS model also with no relay nodes under the assumption that all the other alive nodes are used to repair a failed one, which maximizes the system capacity as proven in [28]. However, this led to high *reconstruction read cost* which was defined in [17] as the number of helper nodes to recover a failed one. It would be practical and flexible to consider the cluster DSS model where the number of helper nodes is not restricted to the maximum. Although the system capacity would be smaller, we gain more flexibility in the repair process. For example, multiple node failures can be analysed under flexible repair constrains, which was also considered in [1].

In our earlier paper [31], we analysed the capacity of the cluster DSS model under more flexible constraints, where the newcomer did not have to download data from all the other alive nodes. In addition, the storage servers (nodes) and networks vary in realistic storage systems, which is the motivation for researching heterogeneous DSSs [36], [26]. As a general model for cluster DSSs, it is practical to consider the CSN-DSS model [18], [36], which is instructive for construct efficient coding scheme adaptive to various networks. In [31], we introduced and analysed partly the CSN-DSS model. However, the properties of CSN-DSSs are not investigated in detail. The final system capacity and tradeoff with separate nodes are not characterized either, which will be formulated in the present paper.

J. Wang, T. Wang and Y. Luo are with the Department of Computer Science and Engineering, Shanghai Jiao Tong University, Shanghai, 200240, China. Email: {wangzhe.90, wth19941018, yuanluo}@sjtu.edu.cn

Kenneth W. Shum is with the Institute of Network Coding, The Chinese University of Hong Kong, Shatin, New Territories, Hong Kong. Email: wksyum@inc.cuhk.edu.hk

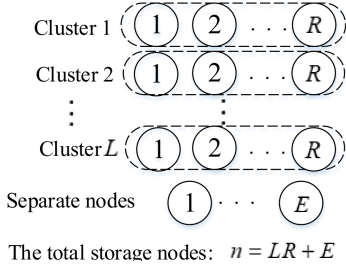


Fig. 1: The CSN-DSS system model

In Section II, the CSN-DSS model is introduced, where the capacity and tradeoff problems are formulated. In Section III, we sketch the properties of cluster DSSs proved in [31], which are also useful in analysing CSN-DSSs. The main contributions of this paper are as follows. The CSN-DSS model is analysed in Section IV, where we prove the applicability of Algorithm 1 and 2 when adding a separate node in Theorem 1. When the location of the added separate node varies, the capacity is analysed in Theorem 2. Consequently, the final capacity of the CSN-DSS model is derived in Theorem 3. Afterward, the tradeoffs between node storage and repair bandwidth are characterized for the cluster DSS and CSN-DSS models in Section V. Based on the tradeoff bounds, a regenerating code construction for the CSN-DSS model is investigated in Section VI. In Section VII, we analyse the influence of adding a separate node to the system capacity theoretically. We prove that adding a separate node will reduce or keep the capacity of a cluster DSS, depending on the system node parameters.

II. PRELIMINARIES

A. The model of distributed storage system with clusters and separate nodes (CSN-DSS)

As Figure 1 shows, the CSN-DSS model consists of $n = LR + E$ storage nodes in total (L clusters and E separate nodes). Each cluster contains R nodes. Assume the original data of size M are encoded with erasure coding and stored in n nodes each of size α . The n nodes satisfy the (n, k) MDS¹ property meaning that any k nodes out of n suffice to reconstruct the original data. When a node fails, there are two types of repair pattern: *exact repair* and *functional repair*. In exact repair, the lost data must be exactly recovered. On the other hand, we only demand the n nodes after each repair keep the MDS property [10] in functional repair. We assume the repair procedure will not change the location of failed nodes. Thus the number of model nodes will not change with node failure and repair. This paper handles the functional repair situation and only considers one node failure.

When repairing a **cluster node**, the newcomer downloads β_I symbols from each of the d_I intra-cluster nodes and β_C symbols from each of the d_C cross-cluster nodes. We define the total number of helper nodes as

$$d \triangleq d_I + d_C.$$

¹Maximum distance separate (MDS) codes achieve optimality in terms of redundancy and error tolerance

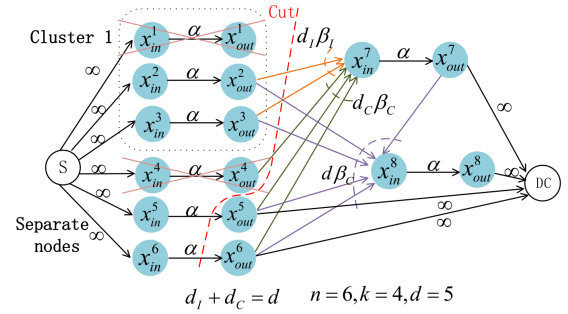


Fig. 2: An IFG of the CSN-DSS model

The same as the restrictions introduced in [24] inequality (1), we also assume $k \leq d \leq n - 1$ in the present paper.

As explained in [31], transmissions among intra-cluster nodes are much cheaper and faster, so it is natural to download more data from intra-cluster nodes and less from cross-cluster nodes, namely, $\beta_I \geq \beta_C$. Moreover, all the intra-cluster nodes are utilized in the repair procedure, namely $d_I = R - 1$ in this paper, since using intra-cluster nodes is efficient and preferential in general cases.

As each separate node can be seen as a special cluster only with one node and all the other nodes are cross-cluster, we assume the newcomer downloads β_C symbols from each of d other nodes to repair a failed **separate node**. Note that only d helper nodes are used no matter where the failed one is.

In the CSN-DSS model, $(\alpha, d_I, \beta_I, d_C, \beta_C)$ and (n, k, L, R, E) are called the **storage/repair** and **node parameters** respectively for simplicity. Additionally, when repairing a fail cluster node, the total intra-cluster and is defined as

$$\gamma_I \triangleq d_I \beta_I.$$

Meanwhile, the cross-cluster bandwidth is defined as

$$\gamma_C \triangleq d_C \beta_C.$$

The total repair bandwidth for a separate node is $\gamma_S \triangleq d \beta_C$. The traditional homogeneous DSS of [9] is retrieved here if $\beta_I = \beta_C$.

B. Information Flow Graph (IFG)

In [9], the performance of DSSs was analysed with the information flow graph (IFG) consisting of three types of nodes: data source S , storage nodes x_{in}^i, x_{out}^i , and data collector DC (see Figure 2). We use x^i to denote a physical storage node represented by a storage input node x_{in}^i and an output node x_{out}^i in the IFG, where data are pre-handled before transmission. The capacity of edge $x_{in}^i \rightarrow x_{out}^i$ is α (the node storage size).

At the initial time, source S emits n edges with infinite capacity to $\{x_{in}^i\}_{i=1}^n$, representing the encoded data are stored in n nodes. Subsequently, S changes to inactive, while the n storage nodes become active. The node x^j ($1 \leq i \leq n$) gets inactive if it has failed. In the failure/repair process, a new node x^{n+1} is added by connecting edges with d active nodes, where the capacity of each edge is β . The value of β varies in the CSN-DSS model (see Figure 2). The IFG

maintains n active nodes after each repair procedure. To keep the (n, k) MDS property, DC selects arbitrary k active nodes to reconstruct the original data, as shown by the edges from k active nodes with infinite capacity.

Figure 2 shows an IFG of the CSN-DSS model, where the cluster node x^1 has failed firstly. Then the newcomer x^7 is created, downloading β_I symbols from each of x^2 and x^3 in cluster 1, and β_C symbols from each of x^4 , x^5 and x^6 out of cluster 1. Subsequently, x^4 is failed, x^8 is generated, connecting with five active nodes.

For an IFG, a (directed) cut between source S and DC is defined as a subset of edges, satisfying the condition that every directed path from S to DC contains at least one edge in the subset. The **min-cut** is the cut between S and DC where the total sum of the edge capacities is smallest [9].

C. Problem Formulation

As introduced in [31], for a CSN-DSS model with (n, k, L, R, E) , the main problem is to characterize the feasible region of points $(\alpha, d_I, \beta_I, d_C, \beta_C)$ to store file of size M reliably. Similarly to [9], this problem is solved through analysing the min-cuts of all possible IFGs corresponding to this CSN-DSS model. According to the max flow bound [3], [21] in network coding, to ensure reliable storage, the file size M will not greater than the system **capacity**

$$\mathbb{C} \triangleq \text{min-cut of } G^*,$$

where G^* is the IFG with the minimum min-cut. That is to say

$$\mathbb{C} \geq M \quad (1)$$

need to be satisfied, which was also proved in [9]. When the node parameters are given, \mathbb{C} is obtained as a function of $(\alpha, d_I, \beta_I, d_C, \beta_C)$. Thus the tradeoff between α and $(d_I, \beta_I, d_C, \beta_C)$ can be derived.

D. Terminologies and Definitions

In this subsection, we introduce some terms defined in [31] to investigate the capacity of the CSN-DSS model through analyse the min-cuts of the corresponding IFGs.

Topological ordering and the min-cut: As introduced in [5], the topological ordering of vertices in a directed acyclic graph is an ordering that if there exists a path from v_i to v_j then $i < j$. We use $\{x_{out}^{t_i}\}_{i=1}^k$ to denote the k topologically ordered nodes connecting to DC . As proven in [9], the minimum min-cut is achieved when nodes $\{x_{out}^{t_i}\}_{i=1}^k$ are all newcomers and x^{t_i} connect to all the $i-1$ nodes $\{x^{t_j}\}_{j=1}^{i-1}$. In the CSN-DSS model, to find the minimum min-cut, we also assume that x^{t_i} connect to all the former nodes $\{x^{t_j}\}_{j=1}^{i-1}$, which was also proved in [28].

The **min-cut** can be obtained by cutting $\{x^{t_i}\}_{i=1}^k$ one by one in the topological ordering, which is analysed in Subsection II-E. In fact, when cutting x^{t_i} , since the k output nodes connect to DC with edges of infinite capacity, we only need to compare the capacity of edge $x_{in}^{t_i} \rightarrow x_{out}^{t_i}$ and the total capacity of the edges emanating to $x_{in}^{t_i}$. Then we choose the minor one for cutting, which is called a **part-cut value**.

For instance, the data collector connects to $x_{out}^6, x_{out}^5, x_{out}^7, x_{out}^8$ in Figure 2, which are topologically ordered. Assume that the red dashed line is the final cut

line. In this case, when cutting x^7 , we need to compare the capacity of edge $x_{in}^7 \rightarrow x_{out}^7$ and the total capacity of the edges emanating to x_{in}^7 , where the latter one is minor if $2\beta_I + \beta_C \leq \alpha$. Note that, not all the edges emanating to x_{in}^7 are cut and counted in the part-cut value, which depends on the topological ordering analysed in Subsection II-E. On the other hand, if $2\beta_I + \beta_C > \alpha$, the cut line will cross the edge $x_{in}^7 \rightarrow x_{out}^7$ and the part-cut value will be α . When all the k nodes connecting to DC are cut, the min-cut is calculated by summing the k part-cut values (see formula (5)).

Repair sequence and selected nodes: The topological ordering of k output nodes $\{x_{out}^{t_i}\}_{i=1}^k$ corresponds to a **repair sequence** of original nodes which are called **selected nodes**. For example, the numbered nodes in Figure 3 are 7 selected nodes where the numbers indicate a repair sequence. In homogeneous distributed storage systems [9], the storage nodes are undifferentiated, thus the min-cuts are independent of repair sequences. However, due to the heterogeneity of intra-cluster and cross-cluster bandwidths in the CSN-DSS model, various repair sequences lead to different min-cuts, and we represent the repair sequence with following definitions.

Selected node distribution and cluster order: For a CSN-DSS model with (n, k, L, R, E) , we relabel the clusters by the amount of selected nodes in a non-increasing order without loss of generality. For example, in Figure 3, cluster 1 contains 3 selected nodes (the most) and cluster 3 contains 0 selected nodes (the least). The **selected node distribution** is denoted with $\mathbf{s} = (s_0, s_1, \dots, s_L)$, where s_0 is the amount of separate selected nodes, and s_i ($1 \leq i \leq L$) represents the amount of selected nodes in cluster i . Meanwhile, the set of all possible selected node distributions is denoted as

$$\mathcal{S} \triangleq \left\{ \mathbf{s} = (s_0, s_1, \dots, s_L) : s_{i+1} \leq s_i, 0 \leq s_i \leq R, \right. \\ \left. \text{for } 1 \leq i \leq L; 0 \leq s_0 \leq S; \sum_{i=0}^L s_i = k \right\}.$$

Additionally, the **repair sequence** is represented by the **cluster order** $\boldsymbol{\pi} = (\pi_1, \pi_2, \dots, \pi_k)$, where π_i ($1 \leq i \leq k$) equals the index of the cluster containing newcomer x^{t_i} . We set $\pi_i = 0$ when node i is separate. As the nodes in one cluster are undifferentiated, we only need to record the cluster index. For a certain $\mathbf{s} = (s_0, s_1, s_2, \dots, s_L)$, the set of all possible cluster orders is specified as

$$\Pi(\mathbf{s}) \triangleq \left\{ \boldsymbol{\pi} = (\pi_1, \dots, \pi_k) : \sum_{j=1}^k \mathbb{I}(\pi_j = i) = s_i \text{ for } 0 \leq i \leq L \right\},$$

where

$$\mathbb{I}(\pi_j = i) = \begin{cases} 1, & \text{if } \pi_j = i, \\ 0, & \text{otherwise.} \end{cases}$$

In Figure 3, $\mathbf{s} = (1, 3, 3, 0)$ represents that the DC connects one separate node and the nodes from cluster 1, 2 and 3 are 3, 3, 0 respectively. Meanwhile, a possible cluster order for \mathbf{s} is $\boldsymbol{\pi} = (1, 1, 1, 2, 2, 2, 0)$, indicated by the numbers from 1 to 7. As Figure 3 shows, the k selected nodes are numbered sequentially for convenience. Additionally, the cluster nodes are

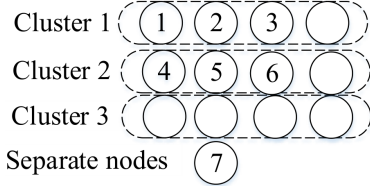


Fig. 3: For a CSN-DSS model, the selected node distribution is $\mathbf{s} = (1, 3, 3, 0)$ and the cluster order $\boldsymbol{\pi} = (1, 1, 1, 2, 2, 2, 0)$ as the numbered nodes show.

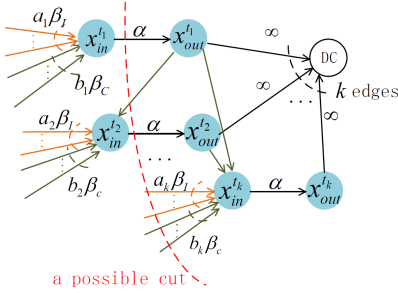


Fig. 4: Calculating the min-cut value

also ordered column by column cross clusters, for simplicity of description, we also say that node 1 and 4 are in the first column of the model, node 2 and 5 are in the second column, and node 3 and 6 are in the third column, meaning that the columns of cluster nodes are labeled by 1 to R from left to right implicitly. These descriptions are used in the following sections.

Moreover, for a given cluster order $\boldsymbol{\pi}$, assume node i is the $h_{\boldsymbol{\pi}}(i)$ -th one in its own cluster, where we define the **relative location** of node i as

$$h_{\boldsymbol{\pi}}(i) \triangleq \sum_{j=1}^i \mathbb{I}(\boldsymbol{\pi}_j = \boldsymbol{\pi}_i), \quad (2)$$

for $1 \leq i \leq k$. Note that the **relative location** specifies the precedence of selected nodes in each cluster. It is obvious that node i is in the $h_{\boldsymbol{\pi}}(i)$ -th column. For instance, Figure 3 illustrates $\boldsymbol{\pi} = (1, 1, 1, 2, 2, 2, 0)$ and the corresponding $h_{\boldsymbol{\pi}}(i)$ sequence $(1, 2, 3, 1, 2, 3, 1)$ calculated with (2). For node 3, $h_{\boldsymbol{\pi}}(3) = \mathbb{I}(\boldsymbol{\pi}_1 = \boldsymbol{\pi}_3) + \mathbb{I}(\boldsymbol{\pi}_2 = \boldsymbol{\pi}_3) + \mathbb{I}(\boldsymbol{\pi}_3 = \boldsymbol{\pi}_3) = 1 + 1 + 1 = 3$ where $\boldsymbol{\pi}_3 = 1$, and therefore node 3 is in the third column.

E. Calculating the min-cut value

As explained in Subsection II-D, for given \mathbf{s} and $\boldsymbol{\pi}$, the min-cut value is obtained by calculate the k part-cut values step by step. When calculating the i -th part-cut value, we define the i -th part incoming weight with formula (4). The final min-cut value is obtained by formula (5).

As introduced in [9], [31], after cutting the k topologically ordered nodes $\{x^{t_i}\}_{i=1}^k$ (see Figure 4) iteratively, the nodes of the IFG G are divided into two disjoint sets V and \bar{V} . The min-cut (denoted by \mathcal{U}) is the set of edges emanating from V to \bar{V} . In the beginning, V consists of source S and the original nodes $x^i (1 \leq i \leq n)$, and \bar{V} consists of DC . When cutting

node $x^{t_i} (1 \leq i \leq k)$, $x_{in}^{t_i}$ and $x_{out}^{t_i}$ are included to V or \bar{V} based on the following process.

Step 1: When considering node x^{t_1} , the first topologically ordered node, there are two possible cases.

- If $x_{in}^{t_1} \in V$, the edge $x_{in}^{t_1} \rightarrow x_{out}^{t_1}$ must be in \mathcal{U} and the first part-cut value is α .
- If $x_{in}^{t_1} \in \bar{V}$, since there are $d = d_I + d_C$ incoming edges for node $x_{in}^{t_1}$, the topologically first node in \bar{V} , all the d edges must be contained by \mathcal{U} , consisting of d_I and d_C edges from intra-cluster and cross-cluster nodes respectively. In this case, the part-cut value is $d_I \beta_I + d_C \beta_C$.

Step 2: Now consider node $x^{t_i} (1 \leq i \leq k)$:

- If $x_{in}^{t_i} \in V$, edge $x_{in}^{t_i} \rightarrow x_{out}^{t_i}$ should be in \mathcal{U} .
- If $x_{in}^{t_i} \in \bar{V}$, the $d = d_I + d_C$ incoming edges of node $x_{in}^{t_i}$ consist of edges from V and \bar{V} respectively. And only the edges from V are contained by \mathcal{U} .
 - If x^{t_i} is in a cluster, among the incoming edges from V , we use a_i and b_i to represent the number of edges **from intra-cluster** and **cross-cluster** nodes respectively. Obviously, we have $0 \leq a_i \leq d_I$ and $0 \leq b_i \leq d_C$. As x^{t_i} connect to all the former $\{x^{t_j}\}_{j=1}^{i-1}$ nodes (introduced in Subsection II-D), when i increases by 1, either a_i or b_i will decrease by 1 until either one reduced to 0, depending on the locations of $\{x^{t_j}\}_{j=1}^i$.
 - If x^{t_i} is separate, c_i represents the number of incoming edges from V . Since $d \geq k$ and $1 \leq i \leq k$, it is obvious that

$$c_i = d - (i - 1). \quad (3)$$

For given \mathbf{s} and $\boldsymbol{\pi}$, the i -th **part incoming weight** is defined as

$$w_i(\mathbf{s}, \boldsymbol{\pi}) \triangleq \begin{cases} a_i(\mathbf{s}, \boldsymbol{\pi})\beta_I + b_i(\mathbf{s}, \boldsymbol{\pi})\beta_C, & \text{node } i \text{ is in a cluster,} \\ c_i(\mathbf{s}, \boldsymbol{\pi})\beta_C, & \text{node } i \text{ is separate} \end{cases} \quad (4)$$

When \mathbf{s} is fixed, we also write $w_i(\mathbf{s}, \boldsymbol{\pi})$ as $w_i(\boldsymbol{\pi})$ for simplicity. Meanwhile, we also use $a_i(\boldsymbol{\pi})$, $b_i(\boldsymbol{\pi})$, $c_i(\boldsymbol{\pi})$ for specific $\boldsymbol{\pi}$.

Subsequently, the min-cut for the given \mathbf{s} and $\boldsymbol{\pi}$ is obtained as

$$MC(\mathbf{s}, \boldsymbol{\pi}) = \sum_{i=1}^k \min\{\alpha, w_i(\mathbf{s}, \boldsymbol{\pi})\}. \quad (5)$$

The capacity of a given CSN-DSS model can be obtained by comparing the min-cuts of IFGs corresponding to selected node distributions $\mathbf{s} \in \mathcal{S}$ and cluster orders $\boldsymbol{\pi} \in \Pi(\mathbf{s})$. In Section III, we will sketch the main results of the capacity of the cluster DSS model, analysed in [31] in detail.

III. THE CAPACITY OF THE CLUSTER DSS MODEL

In [31], we investigated the capacity of the cluster DSS model. The main results are sketched in this section, which are generalized to the CSN-DSS model in Section IV and compared with CSN-DSSs in Section V and VII. For a cluster DSS model with $(n, k, L, R, E = 0)$, the min-cuts of all possible IFGs are compared in two steps on $\boldsymbol{\pi}$ and \mathbf{s} , corresponding to the **vertical order algorithm** and **horizontal selection algorithm** respectively.

- **Step 1:** Fix the selected node distribution \mathbf{s} , we analyse the min-cuts for various $\boldsymbol{\pi} \in \Pi(\mathbf{s})$ in Proposition 1. The vertical order algorithm is named accordingly because the values of cluster order is generated among the clusters alternately, seeming vertically generated in Figure 5.
- **Step 2:** Fix the cluster order generating algorithm, we analyse the min-cuts for different \mathbf{s} in Proposition 2. The horizontal selection algorithm is named accordingly because the output values is generated by selecting the nodes in one cluster until no nodes left. Then select from the next cluster until there are k selected nodes, see Figure 5.

A. Vertical order algorithm for $d_I = R - 1$

For a cluster DSS model with $(n, k, L, R, E = 0)$, Proposition 1 specifies the cluster order $\boldsymbol{\pi}$ minimizing the min-cut $MC(\mathbf{s}, \boldsymbol{\pi})$ for an arbitrary selected node distribution \mathbf{s} . As introduced in [31], the authors of [27], [28] proposed this algorithm under the assumption that the number of helper nodes is $n - 1$, namely, $d_I = R - 1$ and $d_C = n - R$, which maximizes the system capacity as proven in [28]. However, this assumption leads to high reconstruction read cost (all alive nodes are used), which was defined in [17] as the number of helper nodes to recover a failed one. We analysed the algorithm in more general cases with new methods in [31]. The number of cross-cluster helper nodes, d_C , satisfies

$$k - R + 1 \leq d_C \leq n - R \quad (6)$$

and does not have to be $n - R$ of the constraint in [27], which follows from the condition that $k \leq d_I + d_C \leq n - 1$ and $d_I = R - 1$.

Algorithm 1 Vertical order algorithm in the CSN-DSS model

Input: Selected node distribution $\mathbf{s} = (s_0, s_1, \dots, s_L)$.

Output: Cluster order $\boldsymbol{\pi}^* = (\pi_1^*, \dots, \pi_k^*)$.

- 1: Initial cluster label $j \leftarrow 1$;
 - 2: **for** $i = 1$ to k **do**
 - 3: **if** the i -th selected node is a separate node **then**
 - 4: $\pi_i^* \leftarrow 0$; *continue*;
 - 5: **end if**
 - 6: **if** $s_j = 0$ **then**
 - 7: $j = 1$;
 - 8: **else**
 - 9: $\pi_i^* \leftarrow j$; $s_j \leftarrow s_j - 1$; $j \leftarrow (j \bmod L) + 1$;
 - 10: **end if**
 - 11: **end for**
-

In Figure 5, the cluster order $\boldsymbol{\pi}^* = (1, 2, 1, 2, 1, 0, 1)$ is assigned vertically from the first to the fourth column, as the selected node number shows. For given \mathbf{s} and $\boldsymbol{\pi}$, $MC(\mathbf{s}, \boldsymbol{\pi})$ is obtained by (5), which is calculated with

$$w_i(\boldsymbol{\pi}) = a_i(\boldsymbol{\pi})\beta_I + b_i(\boldsymbol{\pi})\beta_C \quad (1 \leq i \leq k).$$

We proof a property for $a_i(\boldsymbol{\pi})$ (the coefficient of β_I) in Lemma 1, which can also be used to calculate $a_i(\boldsymbol{\pi})$.

Lemma 1 ([31]). *For a cluster DSS model, when the selected node distribution $\mathbf{s} = (s_0, s_1, \dots, s_L)$ is fixed, the elements of*

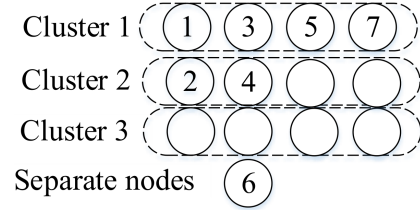


Fig. 5: The cluster order $\boldsymbol{\pi}^* = (1, 2, 1, 2, 1, 0, 1)$ and selected node distribution $\mathbf{s}^* = (1, 4, 2, 1)$ are generated by Algorithm 1 and 2.

*multi-set*² $[a_i(\boldsymbol{\pi})]_{i=1}^k = [a_1(\boldsymbol{\pi}), \dots, a_k(\boldsymbol{\pi})]$ for each cluster order $\boldsymbol{\pi} \in \Pi(\mathbf{s})$ are the same. Additionally, $a_i(\boldsymbol{\pi}) = d_I + 1 - h_{\boldsymbol{\pi}}(i)$ for $1 \leq i \leq k$.

Proposition 1 ([31]). *For a cluster DSS model and any fixed $\mathbf{s} \in \mathcal{S}$, the cluster order $\boldsymbol{\pi}^*$ generated by Algorithm 1 minimizes the min-cut, meaning that*

$$MC(\mathbf{s}, \boldsymbol{\pi}^*) \leq MC(\mathbf{s}, \boldsymbol{\pi})$$

holds for any $\boldsymbol{\pi} \in \Pi(\mathbf{s})$.

We use

$$\boldsymbol{\pi}^*(\mathbf{s}) = (\pi^*(\mathbf{s})_1, \pi^*(\mathbf{s})_2, \dots, \pi^*(\mathbf{s})_k) \quad (7)$$

to represent **the output cluster order** of Algorithm 1 for any input $\mathbf{s} \in \mathcal{S}$. Subsequently, Subsection III-B analyse the min-cuts corresponding to $\boldsymbol{\pi}^*(\mathbf{s})$ for various $\mathbf{s} \in \mathcal{S}$.

B. Horizontal selection algorithm for $d_I = R - 1$

For the selected node distributions $\mathbf{s} \in \mathcal{S}$, we compare the min-cuts corresponding to cluster orders $\boldsymbol{\pi}^*(\mathbf{s})$ and prove that $\boldsymbol{\pi}^*(\mathbf{s}^*)$ minimizes the min-cut in Proposition 2, where $\mathbf{s}^* = (s_0^*, \dots, s_L^*)$ is obtained by Algorithm 2. As introduced before, the cluster order generating algorithm is fixed for different \mathbf{s} .

Algorithm 2 Horizontal selection algorithm in the CSN-DSS model

Input: Node parameters: (n, k, L, R, E) .

Output: Selected node distribution $\mathbf{s}^* = (s_0^*, s_1^*, \dots, s_L^*)$.

- 1: $s_0^* \leftarrow E$
 - 2: **for** $i = 1 \rightarrow L$ **do**
 - 3: **if** $i \leq \lfloor \frac{k-s_0^*}{R} \rfloor$ **then** $s_i^* \leftarrow R$
 - 4: **end if**
 - 5: **if** $i = \lfloor \frac{k-s_0^*}{R} \rfloor + 1$ **then** $s_i^* \leftarrow k - s_0^* - \lfloor \frac{k-s_0^*}{R} \rfloor R$
 - 6: **end if**
 - 7: **if** $i > \lfloor \frac{k-s_0^*}{R} \rfloor + 1$ **then** $s_i^* \leftarrow 0$
 - 8: **end if**
 - 9: **end for**
-

As introduced in [31], when $s_0^* = E = 0$, this algorithm reduces to the cluster version ($d = n - 1$) proposed in [27]. We also analyse this algorithm under more general assumptions as introduced in Subsection III-A. Additionally, we generalize

²The multi-set is a general definition of set, allowing multiple instances of its elements.

the horizontal selection algorithm to the CSN-DSS model with $s_0^* = 1$, which is analysed in Section IV. Figure 5 shows an example for Algorithm 2, where $k = 7$, $R = 4$ and $s_0^* = 1$, thus $s_1^* = 4$, $s_2^* = k - s_0^* - \lfloor \frac{k-s_0^*}{R} \rfloor R = 6 - 4 = 2$. Subsequently, a property of $a_i(\pi^*(s^*))$ and $b_i(\pi^*(s^*))$, the coefficients of β_I and β_C , is proved in Lemma 2.

Lemma 2 ([31]). *For a cluster DSS model, the coefficients of β_I and β_C satisfy*

$$a_i(\pi^*(s^*)) + b_i(\pi^*(s^*)) = d_I + d_C + 1 - i, \quad (8)$$

for $1 \leq i \leq k$, where s^* is generated by Algorithm 2, and $\pi^*(\cdot)$ is defined by (7).

Proposition 2 ([31]). *For a cluster DSS model, cluster order $\pi^*(s^*)$ minimizes the min-cut, meaning that*

$$MC(s^*, \pi^*(s^*)) \leq MC(s, \pi^*(s))$$

holds for all $s \in \mathcal{S}$ with $s_0 = 0$, where s^* is generated by Algorithm 2 and $\pi^*(\cdot)$ is defined by (7).

As introduced in Subsection II-C, the capacity of cluster DSSs is the minimum min-cut which is achieved by $\pi^*(s^*)$ and s^* generated by Algorithm 1 and 2. Note that, the algorithms are also applicative to analyse the capacity of CSN-DSSs with one separate node, which will be investigated in the following Section IV.

IV. THE CAPACITY OF CSN-DSSS

As introduced in Section III, the capacity of the cluster DSS model is achieved by cluster order $\pi^*(s^*)$ generated with Algorithm 1, where s^* is generated by Algorithm 2. In this section, we first analyse the min-cuts corresponding to cluster orders with one separate node in Theorem 1, where the applicability of Algorithm 1 and 2 is proved. Subsequently, when the location of the added separate node varies, the corresponding min-cuts are analysed in Theorem 2, with which the capacity of the CSN-DSS model is formulated in Theorem 3 finally.

In Theorem 1, we assume the separate node is at any given location j ($1 \leq j \leq k$) in every cluster orders and compare the min-cuts combining the two aspects corresponding to Proposition 1 and Proposition 2.

Theorem 1. *For a CSN-DSS model with the separate selected node at location j ($1 \leq j \leq k$), the cluster order $\pi^*(s^*)$ minimizes the min-cut, meaning that*

$$MC(s^*, \pi^*(s^*)) \leq MC(s, \pi), \quad (9)$$

holds for all $s \in \mathcal{S}$ with $s_0 = 1$ and $\pi \in \Pi(s)$ with $\pi_j = 0$, where s^* is generated by Algorithm 2 and $\pi^*(\cdot)$ is defined by (7).

Proof. In [31], we sketch the main idea of this proof, which will be completed here. We will reduce this proof to Proposition 1 and Proposition 2. As the j -th selected node is separate and fixed for each π , we only need to consider the part of selected cluster nodes by analysing the influence of adding a separate selected node. It is convenient to represent the

cluster order π with another cluster order $\bar{\pi}$ without separate nodes, as formula (24) shows (see Figure 12 (b), (c)). The part incoming weights $w_i(\pi)$ ($1 \leq i \leq k$) are then expressed with $w_i(\bar{\pi})$, and this theorem is proved by analysing $w_i(\bar{\pi})$ with similar methods used in Proposition 1 and 2. See A for more details. \square

Remark 1. *After adding a separate selected node, other $k - 1$ selected cluster nodes generated by Algorithm 1 and 2 are ordered similarly to the situation without separate nodes. It can be verified that Lemma 1 and Lemma 2 still hold for the cluster selected nodes in the CSN-DSSs with one separate node. The added separate node will not influence the properties of the other $k - 1$ cluster selected nodes, which can be proved with the same methods to Lemma 1 and Lemma 2. We omit these proofs due to space limitation and use Lemma 1 and Lemma 2 directly.*

In order to analyse the relationship between the min-cuts and the separate selected node location, let MC_j^* denote the min-cut corresponding to s^* and $\pi^*(s^*)$ mentioned in Theorem 1, where $s_0^* = 1$ and $\pi^*(s^*)_j = 0$, namely,

$$MC_j^* \triangleq MC(s^*, \pi^*(s^*)) \quad (10)$$

for $1 \leq j \leq k$. The corresponding cluster order is represented with $\pi^{(j)}$, namely,

$$\pi^{(j)} \triangleq \pi^*(s^*) \text{ with } \pi^*(s^*)_j = 0. \quad (11)$$

Remark 2. *Note that the separate selected node location is not identified by $\pi^*(s^*)$ explicitly. For notational simplicity, we use $\pi^*(s^*)$ to denote the cluster order without separate nodes if not explicitly state. On the other hand, let $\pi^{(j)}$ denote the cluster order with one separate selected node at location j . Both $\pi^*(s^*)$ and $\pi^{(j)}$ are generated by Algorithm 1 and 2.*

Subsequently, we compare min-cuts MC_j^* and MC_{j+1}^* and prove that $MC_j^* \geq MC_{j+1}^*$ for $1 \leq j \leq k - 1$ in the following Theorem 2, with which the final capacity of the CSN-DSS model is derived in Theorem 3.

Theorem 2. *For a CSN-DSS model with one separate node, the min-cuts of IFGs corresponding to the cluster order $\pi^{(j)}$ satisfy that*

$$MC_j^* \geq MC_{j+1}^*,$$

for $1 \leq j \leq k - 1$, where $\pi^{(j)}$ is defined by (11) with the separate node at location j and MC_j^* is defined by (10).

Proof. To prove this theorem, the part incoming weights $w_i(\pi^{(j)})$ and $w_i(\pi^{(j+1)})$ ($1 \leq i \leq k$) are compared one by one. By analysing cluster orders $\pi^{(j)}$ and $\pi^{(j+1)}$, we find that

$$w_i(\pi^{(j)}) = w_i(\pi^{(j+1)})$$

for $i \in [k] \setminus \{j, j + 1\}$ ³. Hence, we only need to compare $w_j(\pi^{(j)})$, $w_{j+1}(\pi^{(j)})$ and $w_j(\pi^{(j+1)})$, $w_{j+1}(\pi^{(j+1)})$. We enumerate all the possible cases of the above four components to complete this proof. See B for more details. \square

³Let $[k]$ denote the integer set $\{1, 2, \dots, k\}$.

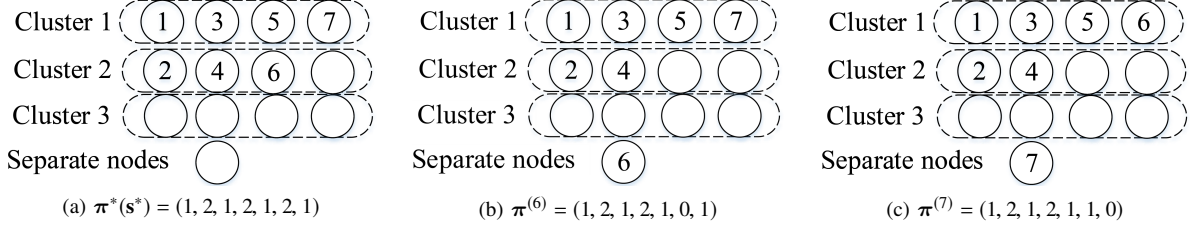


Fig. 6: In (a), the cluster order is $\pi^*(\mathbf{s}^*) = (1, 2, 1, 2, 1, 2, 1)$ for $\mathbf{s}^* = (0, 4, 3)$. In (b) and (c), the cluster orders $\pi^{(6)}$ and $\pi^{(7)}$ are corresponding to $\mathbf{s} = (1, 4, 3, 0)$, where the separate selected node locations are 6 and 7, respectively.

With Theorem 2, the minimum min-cut with one separate selected node is derived. We obtain the capacity of the CSN-DSS model in Theorem 3 through comparing MC_j^* and $MC(\mathbf{s}^*, \pi^*(\mathbf{s}^*))$, where $\pi^*(\mathbf{s}^*)$ without the separate node is generated by Algorithm 1 and 2, as introduced in Remark 2.

Theorem 3. For a CSN-DSS model with one separate node, the system capacity is

$$MC_k^* = \sum_{i=1}^k \min \{w_i(\pi^{(k)}), \alpha\},$$

where $\pi^{(k)}$ is defined by (11).

Proof. As proven in Theorem 2, MC_k^* is the minimum min-cut with one separate selected node. Proposition 2 proves that $MC(\mathbf{s}^*, \pi^*(\mathbf{s}^*))$ is the minimum min-cut corresponding to cluster orders without separate nodes. Hence, we only need to compare MC_k^* and $MC(\mathbf{s}^*, \pi^*(\mathbf{s}^*))$.

For the cluster order $\pi^*(\mathbf{s}^*)$ without separate nodes, we can always find a cluster order $\pi^{(j)}$ with one fixed separate selected node at location j , satisfying that

$$\pi^*(\mathbf{s}^*)_t = \pi^{(j)}_t, \quad (12)$$

for $1 \leq t \leq k$ and $t \neq j$, where $j = k - \lfloor \frac{k}{R} \rfloor$. Then

$$w_t(\pi^*(\mathbf{s}^*)) = w_t(\pi^{(j)}), \quad (13)$$

for $1 \leq t \leq k$ and $t \neq j$. When $t = j$,

$$\begin{aligned} w_j(\pi^*(\mathbf{s}^*)) &= a_j(\pi^*(\mathbf{s}^*))\beta_I + b_j(\pi^*(\mathbf{s}^*))\beta_C \\ &\stackrel{(a)}{\geq} (a_j(\pi^*(\mathbf{s}^*)) + b_j(\pi^*(\mathbf{s}^*)))\beta_C \\ &\stackrel{(b)}{=} (d_I + d_C + 1 - j)\beta_C = w_j(\pi^{(j)}), \end{aligned}$$

where (a) is because of $\beta_I \geq \beta_C$ and (b) is based on Lemma 2. Hence,

$$MC(\mathbf{s}^*, \pi^*(\mathbf{s}^*)) \geq MC_j^*.$$

Then $MC_k^* \leq MC_j^* \leq MC(\mathbf{s}^*, \pi^*(\mathbf{s}^*))$.

As shown in Figure 6, for the cluster order $\pi^*(\mathbf{s}^*) = (1, 2, 1, 2, 1, 2, 1)$ in (a), we can find a cluster order $\pi^{(6)} = (1, 2, 1, 2, 1, 0, 1)$ in (b) with the separate node at location $j = k - \lfloor \frac{k}{R} \rfloor = 7 - \lfloor \frac{7}{4} \rfloor = 6$, satisfying condition (12). Additionally, $w_6(\pi^*(\mathbf{s}^*)) = (d_I - 2)\beta_I + (d_C - 3)\beta_C \geq (d_I + d_C - 5)\beta_C = w_6(\pi^{(6)})$. Hence, $MC_6^* \leq MC(\mathbf{s}^*, \pi^*(\mathbf{s}^*))$. In Figure 6 (c), the locations of separate selected nodes is $k = 7$. Based on Theorem 2, $MC_7^* \leq MC_6^*$. Then $MC_7^* \leq MC_6^* \leq MC(\mathbf{s}^*, \pi^*(\mathbf{s}^*))$. \square

V. TRADEOFFS FOR THE CSN-DSS AND CLUSTER DSS MODEL

In Theorem 3, the capacity of a CSN-DSS model with one separate node is specified as MC_k^* , the left part of formula (14). As introduced in Subsection II-C, by analysing

$$\sum_{i=1}^k \min \{w_i(\pi^{(k)}), \alpha\} \geq \mathcal{M}, \quad (14)$$

the tradeoff bound between node storage α and repair bandwidth parameters $(d_I, \beta_I, d_C, \beta_C)$ will be characterized, which is figured out in formula (16) and calculated with formula (15).

Let $w_i^* \triangleq w_i(\pi^{(k)})$ for simplicity and w_i^* can be figured out as

$$w_{k-i+1}^* = \begin{cases} \left(R - \left\lfloor \frac{i}{\lfloor \frac{k-1}{R} \rfloor + 1} \right\rfloor \right) \beta_I + \left(d_C - i + \left\lfloor \frac{i}{\lfloor \frac{k-1}{R} \rfloor + 1} \right\rfloor \right) \beta_C, & 1 \leq i \leq \left(\left\lfloor \frac{k-1}{R} \right\rfloor + 1 \right) \left(k - 1 - \left\lfloor \frac{k-1}{R} \right\rfloor R \right) \\ \left(\left\lfloor \frac{k-i-1}{\lfloor \frac{k-1}{R} \rfloor} \right\rfloor \right) \beta_I + \left(d_C + R - i - \left\lfloor \frac{k-i-1}{\lfloor \frac{k-1}{R} \rfloor} \right\rfloor \right) \beta_C, & \left(\left\lfloor \frac{k-1}{R} \right\rfloor + 1 \right) \left(k - 1 - \left\lfloor \frac{k-1}{R} \right\rfloor R \right) < i \leq k - 1 \\ (R + d_C - k)\beta_C, & i = k \end{cases} \quad (15)$$

In formula (15), the subscript of w^* is set as $k - i + 1$ for convenience to ensure

$$w_1^* \leq w_2^* \leq \dots \leq w_k^*$$

which will not change MC_k^* . In fact, we can get $w_2^* \leq \dots \leq w_k^*$ by using Algorithm 1 and 2. In addition, because of Lemma 2 and $\beta_I \geq \beta_C$, we can also find that $w_1^* = (d_I + d_C + 1 - k)\beta_C$ is the minimum among $w_i^* (1 \leq i \leq k)$.

Assume α^* is the minimum α satisfying (14). With similar methods in [31], the tradeoff bound is obtained (See Figure 10 for example). For $i = 2, \dots, k$,

$$\alpha^* = \frac{\mathcal{M} - \sum_{j=1}^{i-1} w_j^*}{k - i + 1}, \quad (16)$$

for $\mathcal{M} \in (\sum_{j=1}^{i-1} w_j^* + (k - i + 1)w_{i-1}^*, \sum_{j=1}^i w_j^* + (k - i)w_i^*]$. When $i = 1$, $\alpha^* = \mathcal{M}/k$ for $\mathcal{M} \in [0, w_1^*]$.

As introduced in [31], the tradeoff bound of cluster DSSs holds the same expression with (16), but the values of w_j^* are found differently as

$$w_{k-i+1}^* = \begin{cases} \left(R - \left\lfloor \frac{i}{\lfloor \frac{k}{R} \rfloor + 1} \right\rfloor \right) \beta_I + \left(d_C - i + \left\lfloor \frac{i}{\lfloor \frac{k}{R} \rfloor + 1} \right\rfloor \right) \beta_C, & 1 \leq i \leq \left(\left\lfloor \frac{k}{R} \right\rfloor + 1 \right) \left(k - \left\lfloor \frac{k}{R} \right\rfloor R \right) \\ \left(\left\lfloor \frac{k-i}{\lfloor \frac{k}{R} \rfloor} \right\rfloor \right) \beta_I + \left(d_C + R - i - \left\lfloor \frac{k-i}{\lfloor \frac{k}{R} \rfloor} \right\rfloor \right) \beta_C, & \left(\left\lfloor \frac{k}{R} \right\rfloor + 1 \right) \left(k - \left\lfloor \frac{k}{R} \right\rfloor R \right) < i \leq k. \end{cases} \quad (17)$$

Remark 3. When $\beta_I = \beta_C$, Equation (15) and (17) both reduce to

$$w_{k-i+1}^* = (R + d_C - i) \beta_C$$

for $1 \leq i \leq k$, according with the tradeoff bounds in [9] without differentiating clusters and separate nodes. Note that we assume all alive nodes in the same cluster with the failed one are used, thus $d = d_I + d_C = R - 1 + d_C$.

Numerical comparisons of tradeoff bounds for CSN-DSSs with and without the separate node are illustrated in Figure 10 in Section VII where we also analyse the differences theoretically. Similarly to the regenerating code constructions mentioned in [10], [13], interference alignment can also be used in the CSN-DSS with one separate node. We gave a code construction example for cluster DSSs without separate nodes in [31]. The construction problem of CSN-DSSs with one separate node is investigated in the following Section VI.

VI. CODE CONSTRUCTIONS FOR CSN-DSSS WITH ONE SEPARATED NODES

Minimum storage regenerating (MSR) code was proposed in [9], indicating the code constructions which achieve the minimum storage point in the optimum tradeoff curve between storage and repair bandwidth. As MSR code is optimal in terms of the redundancy-reliability [9], there are lots of research works on MSR codes [10], [13], [24], [29], [35]. In this section, we use the interference alignment scheme [33] to give an MSR code construction. For example, the point $(\beta_C = 1, \alpha = 2)$ is the minimum storage point of the CSN-DSS model with $(n = 5, k = 3, L = 2, R = 2, E = 1)$ in Figure 7, where the storage/bandwidth parameter constraints are $\beta_I = 2\beta_C, d_I = 1, d_C = 3$. Under the parameter constraints of the CSN-DSS with one separate node in Figure 7, we will introduce an MSR code construction achieving the point $(\beta_C = 1, \alpha = 2)$.

Figure 8 shows the system node configurations, where there are one separate node and 2 clusters each with 2 nodes. We assume the original file consists of $M = 6$ symbols. The encoding and repair procedures are introduced as follows.

Encoding procedure: The original file consists of $M = 6$ symbols represented by $x_1, x_2, x_3, y_1, y_2, y_3$ and stored in

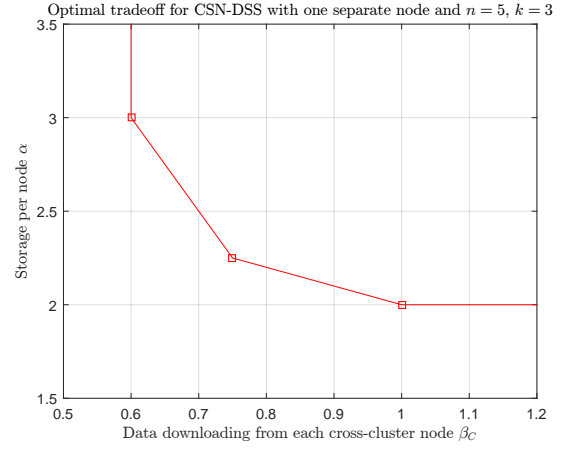


Fig. 7: The optimal tradeoff curve between node storage α and each cross-cluster bandwidth β_C , for the CSN-DSS model, where $\beta_I = 2\beta_C, d_I = 1, d_C = 3$ and $M = 6$.

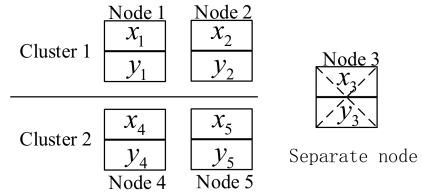


Fig. 8: The code construction illustration for the CSN-DSS model, where $\alpha = 2, \beta_I = 2, \beta_C = 1, d_I = 1, d_C = 3$ and $M = 6$.

node 1, 2 and 3 as Figure 8 shows. We use two $(5, 3)$ -MDS codes to encode (x_1, x_2, x_3) and (y_1, y_2, y_3) respectively. Let

$$\begin{aligned} (x_1, x_2, x_3, x_4, x_5) &= (x_1, x_2, x_3) [\mathbf{I}_{3 \times 3} | \mathbf{A}], \\ (y_1, y_2, y_3, y_4, y_5) &= (y_1, y_2, y_3) [\mathbf{I}_{3 \times 3} | \mathbf{B}], \end{aligned}$$

where $\mathbf{I}_{3 \times 3}$ is an identity matrix. $\mathbf{A} = (a_{ij})_{3 \times 2}$ and $\mathbf{B} = (b_{ij})_{3 \times 2}$ are the encoding matrices. Then

$$\begin{aligned} x_4 &= a_{11}x_1 + a_{21}x_2 + a_{31}x_3, & x_5 &= a_{12}x_1 + a_{22}x_2 + a_{32}x_3, \\ y_4 &= b_{11}y_1 + b_{21}y_2 + b_{31}y_3, & y_5 &= b_{12}y_1 + b_{22}y_2 + b_{32}y_3. \end{aligned}$$

The construction of MSR codes is to find the proper \mathbf{A} and \mathbf{B} satisfying the storage/repair conditions.

Repair procedure: As constrained by the storage/repair parameters, when Node 1 has failed, the newcomer will download $\beta_I = 2$ symbols from Node 2 and $\beta_C = 1$ symbol from each of Node 3, 4 and 5 respectively. On the other hand, when the separate Node 3 has failed, the newcomer will download one symbol from each of the four alive nodes. We first assume the separate Node 3 has failed and the four symbols downloaded from Node 1, 2, 4 and 5 respectively are

$$\begin{aligned} symbol_1 &= c_{11}x_1 + c_{12}y_1 \text{ from Node 1,} \\ symbol_2 &= c_{21}x_2 + c_{22}y_2 \text{ from Node 2,} \\ symbol_4 &= c_{41}x_4 + c_{42}y_4 \text{ from Node 4,} \\ symbol_5 &= c_{51}x_5 + c_{52}y_5 \text{ from Node 5,} \end{aligned}$$

where c_{i1} and c_{i2} ($i = 1, 2, 4, 5$) are called **repair download parameters**, which are designed beforehand to satisfy condition (22). Note that the subscript of *symbol* only represents which cluster it is from. With the equations in the encoding procedure, we get

$$\text{symbol}_1 = c_{11}x_1 + c_{12}y_1, \quad (18)$$

$$\text{symbol}_2 = c_{21}x_2 + c_{22}y_2, \quad (19)$$

$$\begin{aligned} \text{symbol}_4 = & c_{41}a_{11}x_1 + c_{42}b_{11}y_1 + c_{41}a_{21}x_2 + c_{42}b_{21}y_2 \\ & + c_{41}a_{31}x_3 + c_{42}b_{31}y_3, \end{aligned} \quad (20)$$

$$\begin{aligned} \text{symbol}_5 = & c_{51}a_{12}x_1 + c_{52}b_{12}y_1 + c_{51}a_{22}x_2 + c_{52}b_{22}y_2 \\ & + c_{51}a_{32}x_3 + c_{52}b_{32}y_3. \end{aligned} \quad (21)$$

If the coefficients of x_i and y_i ($1 \leq i \leq 3$) in the above 4 equations satisfy that

$$\text{rank} \begin{pmatrix} c_{11} & c_{12} \\ c_{41}a_{11} & c_{42}b_{11} \\ c_{51}a_{12} & c_{52}b_{12} \end{pmatrix} = 1, \quad \text{rank} \begin{pmatrix} c_{21} & c_{22} \\ c_{41}a_{21} & c_{42}b_{21} \\ c_{51}a_{22} & c_{52}b_{22} \end{pmatrix} = 1 \quad (22)$$

and

$$\text{rank} \begin{pmatrix} c_{41}a_{31} & c_{42}b_{32} \\ c_{51}a_{32} & c_{52}b_{32} \end{pmatrix} = 2, \quad (23)$$

we can eliminate x_1, y_1, x_2, y_2 in Eq. 20 and Eq. 21 with Eq. 18 and Eq. 19. Meanwhile, x_3 and y_3 are solved out.

When a cluster node has failed, a similar repair procedure can be executed. As more symbols can be downloaded from intra-cluster nodes, it may be easier to satisfy conditions (22) and (23). In [10], the authors proved that there exist MDS codes and repair download parameters satisfying the condition (22) and (23). The constructions of MDS codes and repair download parameters covering all possible node failures are more complicated. When the system properties of the CSN-DSS with one separate node are considered, the constructions should be easier to find, but more future works are needed.

VII. COMPARISON OF CSN-DSSS WITH AND WITHOUT SEPARATE NODES

In Section V, the tradeoff bounds for CSN-DSSs with and without separate nodes are formulated based on the capacities derived in Section III and Section IV. We will compare the capacity and tradeoff bounds of CSN-DSSs with and without the separate node in this Section VII. The tradeoff bounds of cluster DSSs and those after adding a separate node are illustrated in Figure 10. In Theorem 4, we theoretically prove that when each cluster contains R nodes and any k nodes suffice to reconstruct the original file, adding a separate node will keep the capacity if $R|k$, and reduce the capacity otherwise. Two examples are used to illustrate our main proof ideas. Example 1 shows the situation where the capacity is reduced. Consequently, the tradeoff bounds move left than those without the separate node (see Figure 10 (b)). On the other hand, adding one separate node will not affect the system capacity in Example 2.

Example 1. Figure 9 shows the cluster DSS with ($n = 12, k = 9, L = 3, R = 4, E = 0$) and the CSN-DSS after adding a separate node. The new CSN-DSS model possesses

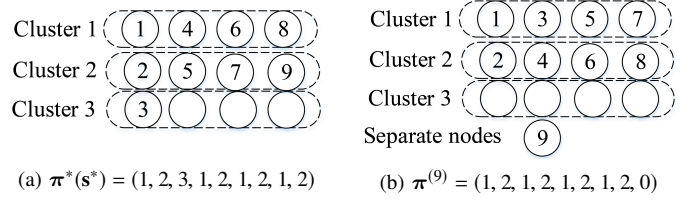


Fig. 9: In (a), the cluster order is $\pi^*(\mathbf{s}^*)$ for $\mathbf{s}^* = (0, 4, 4, 1)$, which achieves the capacity of cluster DSS model. In (b), the cluster order and selected node distribution are $\pi^{(9)}$ and $\mathbf{s}^* = (1, 4, 4, 0)$ respectively, which achieves the capacity of the CSN-DSS model.

the same node and storage/repair parameters except n and E . Based on Theorem 1 and Theorem 3, the cluster orders $\pi^*(\mathbf{s}^*) = (1, 2, 3, 1, 2, 1, 2, 1, 2)$ and $\pi^{(9)} = (1, 2, 1, 2, 1, 2, 1, 2, 0)$ respectively achieve the capacity of these two systems, namely,

$$MC(\mathbf{s}^*, \pi^*(\mathbf{s}^*)) = \sum_{i=1}^k \min \{w_i(\pi^*(\mathbf{s}^*)), \alpha\}$$

and

$$MC_9^* = \sum_{i=1}^k \min \{w_i(\pi^{(9)}), \alpha\}.$$

With the methods of calculating $w_i(\pi)$ (see equation (4)), we compare $w_i(\pi^*(\mathbf{s}^*))$ and $w_i(\pi^{(9)})$ one by one as follows.

- We can verify that $w_i(\pi^*(\mathbf{s}^*)) = w_i(\pi^{(9)})$ for $i = 1, 2$.
- When $i = 4$, although node 4 is in different clusters in Figure 9 (a) and (b), we can get $a_4(\pi^*(\mathbf{s}^*)) = a_4(\pi^{(9)}) = d_I - 1$ (based on Lemma 1) and $b_4(\pi^*(\mathbf{s}^*)) = b_4(\pi^{(9)}) = d_C - 2$ (based on Lemma 2). Then $w_4(\pi^*(\mathbf{s}^*)) = w_4(\pi^{(9)})$. Similarly, we get $w_6(\pi^*(\mathbf{s}^*)) = w_6(\pi^{(9)})$ and $w_8(\pi^*(\mathbf{s}^*)) = w_8(\pi^{(9)})$.
- When $i = 5$, node 5 is in the second column in Figure 9 (a) and in the third column in Figure 9 (b). Based on equation (2) and Lemma 1, $a_5(\pi^*(\mathbf{s}^*)) = d_I - 1 = a_5(\pi^{(9)}) + 1$. Because of Lemma 2, $a_5(\pi^*(\mathbf{s}^*)) + b_5(\pi^*(\mathbf{s}^*)) = d_I + d_C + 1 - 5 = a_5(\pi^{(9)}) + b_5(\pi^{(9)})$, then $b_5(\pi^*(\mathbf{s}^*)) = b_5(\pi^{(9)}) - 1$. Hence, $w_5(\pi^*(\mathbf{s}^*)) - w_5(\pi^{(9)}) = \beta_I - \beta_C \geq 0$. Similarly, $w_3(\pi^*(\mathbf{s}^*)) - w_3(\pi^{(9)}) \geq 0$ and $w_7(\pi^*(\mathbf{s}^*)) - w_7(\pi^{(9)}) \geq 0$.
- When $i = 9$, the 9th selected node is in cluster in Figure 9 (a) and separate in Figure 9 (b). Based on Lemma 1 and Lemma 2, $a_9(\pi^*(\mathbf{s}^*))$ and $w_9(\pi^*(\mathbf{s}^*)) = a_9(\pi^*(\mathbf{s}^*))\beta_I + b_9(\pi^*(\mathbf{s}^*))\beta_C = (d_C - 5)\beta_C$. With equation (3), $w_9(\pi^{(9)}) = (d_I + d_C + 1 - 9)\beta_C = (d_C - 5)\beta_C$. Hence, $w_9(\pi^*(\mathbf{s}^*)) = w_9(\pi^{(9)})$.

Example 1 shows that $w_i(\pi^*(\mathbf{s}^*)) = w_i(\pi^{(9)})$ for $i = 1, 2, 4, 6, 8, 9$ and $w_i(\pi^*(\mathbf{s}^*)) \geq w_i(\pi^{(9)})$ for $i = 3, 5, 7$. Hence, $MC(\mathbf{s}^*, \pi^*(\mathbf{s}^*)) \geq MC_9^*$, and adding one separate node reduces the capacity. Based on equation (17) and (15), the tradeoff bounds are plotted and compared in Figure 10 (b), showing that the tradeoff bounds after adding a separate node move left. As introduced in Subsection II-C and proved in [9], the tradeoff bound is a lower bound for the region of feasible points $(\alpha, d_I, \beta_I, d_C, \beta_C)$ ((α, β_C) in Figure 9) to reliably store

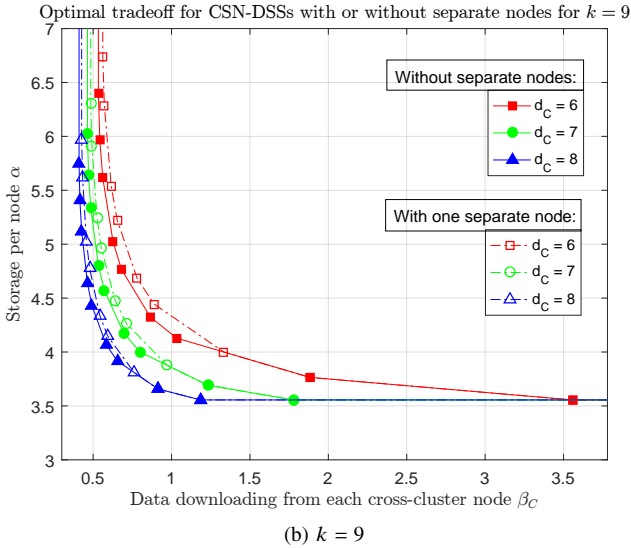
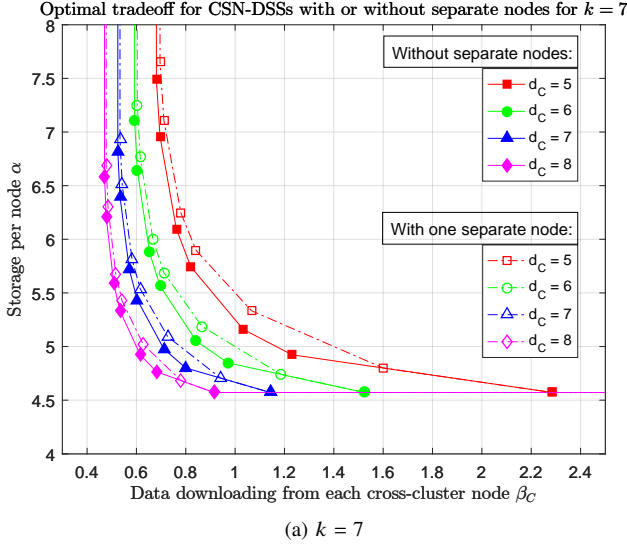


Fig. 10: Optimal tradeoff curves between node storage α and each cross-cluster bandwidth β_C for the cluster DSS model with $(n = 12, k = 7$ or $9, L = 3, R = 4, E = 0)$ and the CSN-DSS model with $(n = 13, k = 7$ or $9, L = 3, R = 4, E = 1)$. The bandwidth constraint is $\tau = \beta_I/\beta_C = 2$ and $\mathcal{M} = 32$. The tradeoff curves are for different numbers of cross-cluster helper nodes d_C respectively. The solid and dotted lines are for the cluster DSS and CSN-DSS models respectively.

the original file of size \mathcal{M} . In this situation, adding one separate node reduces the feasible region of reliable storage points.

Example 2. Figure 11 provides another example where adding a separate node will not change the system capacity. By comparing the selected nodes in $\pi^*(\mathbf{s}^*) = (1, 2, 1, 2, 1, 2, 1, 2)$ and $\pi^{(8)} = (1, 2, 1, 2, 1, 2, 1, 0)$, it is easy to find that the locations of the first 7 selected nodes in Figure 11 (a) are the same to those in Figure 11 (b). Hence, $w_i(\pi^*(\mathbf{s}^*)) = w_i(\pi^{(8)})$ for $1 \leq i \leq 7$ and we only need to compare $w_8(\pi^*(\mathbf{s}^*))$ and

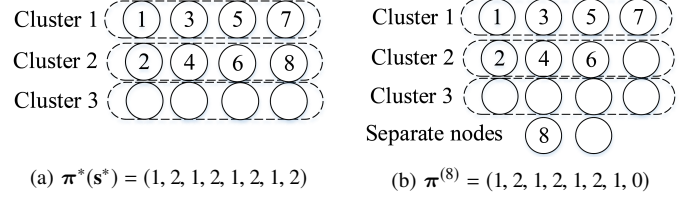


Fig. 11: In (a), the cluster order is $\pi^*(\mathbf{s}^*)$ for $\mathbf{s}^* = (0, 4, 4, 0)$, which achieves the capacity of the cluster DSS model. In (b), the cluster order and selected node distribution are $\pi^{(8)}$ and $\mathbf{s}^* = (1, 4, 4, 0)$ respectively, which achieves the capacity of the CSN-DSS model.

$w_8(\pi^{(8)})$. Based on Lemma 1, Lemma 2 and formula (3),

$$\begin{aligned} w_8(\pi^*(\mathbf{s}^*)) &= (d_I + 1 - h_{\pi^*(\mathbf{s}^*)}(8))\beta_I + (d_I + d_C + 1 - 8 - a_i(\pi^*(\mathbf{s}^*)))\beta_C \\ &= (R + d_C - 7)\beta_C \end{aligned}$$

and

$$w_8(\pi^{(8)}) = (d_I + d_C + 1 - 8)\beta_C = (R + d_C - 7)\beta_C,$$

where $d_I = R - 1$ is given assumptions in this paper, as introduced before. Then, $w_8(\pi^*(\mathbf{s}^*)) = w_8(\pi^{(8)})$. Hence, $MC(\mathbf{s}^*, \pi^*(\mathbf{s}^*)) = MC_8^*$ and adding one separate node will not change the capacity.

Example 1 and Example 2 illustrate that the node parameters decide whether adding one separate node will reduce the system capacity. In Theorem 4, we investigate this problem theoretically.

Theorem 4. *In a cluster DSS model with $(n, k, L, R, E = 0)$ and the CSN-DSS model with $(n + 1, k, L, R, E = 1)$ after adding a new separate node, we assume the storage/bandwidth parameters $(d_I = R - 1, \beta_I, d_C, \beta_C)$ are the same for these two systems, achieving the reliable storage of file with size \mathcal{M} .*

- If node parameters R and k satisfy

$$R \mid k,$$

namely, k is divisible by R , then the new added separate node will not change the capacity.

- If $R \nmid k$, the new added separate node will reduce the capacity of the original cluster DSS model.

Proof. Let $\pi^*(\mathbf{s}^*)$ and $\pi^{(k)}$ denote the cluster orders achieving the capacity of systems with and without the separate node, as shown in Proposition 2 and Theorem 3. Through analysing cluster orders $\pi^*(\mathbf{s}^*)$ and $\pi^{(k)}$, we compare the part incoming weights $[w_i(\pi^*(\mathbf{s}^*))]_{i=1}^k$ and $[w_i(\pi^{(k)})]_{i=1}^k$ one by one and enumerate all possible cases. In the first part, we investigate the case $R \mid k$, where adding a separate node will not change the capacity corresponding to Example 2. In the second part, we consider the case $R \nmid k$, where the system capacity is reduced (see Example 1). See C for more details. \square

Figure 10 (a) and (b) present numerical comparisons between the tradeoff bounds of the cluster DSSs and CSN-DSSs

after adding a separate node. It is shown that the tradeoff bounds move right after adding a separate node, implying that the capacities are reduced for different d_C (the number of helper nodes), when $k = 7, 9$ and other parameters are the same ($M = 32, L = 3, R = 4, \tau = \beta_I/\beta_C = 2$). Additionally, as d_C increases, both of the tradeoff bounds with or without the separate node move left, meaning that the feasible region of the reliable storage points increase, which is consistent with the results in [9] and [31].

In Theorem 4, we prove that adding one separate node will reduce or keep the capacity of a cluster DSS, depending on the relationship of node parameters R and k . This means that when k is fixed, adding a separate node will not improve the system capacity. Additionally, this paper investigates the capacity of CSN-DSSs with one separate node. The capacity of CSN-DSSs with multiple separate nodes can be analysed similarly, but further theoretical proofs are needed.

VIII. CONCLUSIONS

In this paper, we characterize the capacity of the CSN-DSS model with one separate node. The tradeoff bounds of CSN-DSSs are compared with cluster DSSs, which is instructive for construct flexible erasure codes adapting to various network conditions. A regenerating code construction strategy is proposed for the CSN-DSS model, achieving the minimum storage point in the tradeoff bound under specific parameters. The influence of adding a separate node is characterized theoretically. We prove that adding one separate node will reduce or keep the capacity of the cluster DSS model, depending on the system node parameters.

APPENDIX A PROOF OF THEOREM 1

We will reduce this proof to Proposition 1 and Proposition 2. As the separate selected node locations are the same for different π and \mathbf{s} , we only need to consider the part of selected cluster nodes by analysing the influence of adding a separate selected node. It is convenient to represent the cluster order π with another cluster order $\bar{\pi}$ without separate nodes, as formula (24) shows (see Figure 12 (b), (c)). The part incoming weights $w_i(\pi)$ ($1 \leq i \leq k$) are then expressed with $w_i(\bar{\pi})$, and this theorem is proved by analysing $w_i(\bar{\pi})$ with similar methods used in Proposition 1 and 2.

Cluster order assignment: For any cluster order π with a separate selected node (the j -th one), we can always find a cluster order $\bar{\pi} = (\bar{\pi}_1, \bar{\pi}_2, \dots, \bar{\pi}_k)$ without separate selected nodes satisfying that

$$\pi_i = \begin{cases} \bar{\pi}_i, & \text{if } 1 \leq i < j \\ 0, & \text{if } i = j \\ \bar{\pi}_{i-1}, & \text{if } j < i \leq k \end{cases}. \quad (24)$$

Note that the component $\bar{\pi}_k$ will not be used here, thus we only need to analyse the first $k-1$ components of $\bar{\pi}$ actually. The corresponding selected node distributions are denoted by \mathbf{s} and $\bar{\mathbf{s}}$ respectively. For example, in Figure 12 (b), node 3 is separate in $\pi = (1, 2, 0, 1, 2, 1, 2, 3)$ which can be represented

by the cluster order $\bar{\pi} = (1, 2, 1, 2, 1, 2, 3, 1)$ in Figure 12 (c) as $\pi_1 = \bar{\pi}_1, \pi_2 = \bar{\pi}_2, \pi_3 = 0$ and $\pi_i = \bar{\pi}_{i-1}$ ($i = 4, 5, 6, 7, 8$). Figure 12 (a) shows the optimal cluster order π^* and selected node distributions* generated by Algorithm 1 and 2, where the third separate selected node is fixed beforehand.

Based on (4), the part incoming weights for π are

$$w_i(\pi) = \begin{cases} w_i(\bar{\pi}), & \text{if } 1 \leq i < j \\ (d_I + d_C + 1 - i)\beta_C, & \text{if } i = j \\ w_{i-1}(\bar{\pi}) - \beta_C, & \text{if } j + 1 \leq i \leq p \\ w_{i-1}(\bar{\pi}), & \text{if } p + 1 \leq i \leq k \end{cases}, \quad (25)$$

where p is the integer that $b_p(\bar{\pi})$ reduces to 0. As the coefficient of β_C won't be negative, the part incoming weight $w_i(\pi) = w_{i-1}(\bar{\pi}) = a_{i-1}(\bar{\pi})\beta_I$ if $b_{i-1}(\bar{\pi}) = 0$. If $j \geq p$, $w_i(\pi) = w_{i-1}(\bar{\pi})$ for $j + 1 \leq i \leq k$. The value of p varies according to π and $\bar{\pi}$. Let p_{max} denote the maximum value of p for all π and $\bar{\pi}$.

- For the case $j \geq p_{max}$,

$$\begin{aligned} MC(\mathbf{s}, \pi) &= \sum_{i=1}^k \min\{w_i(\pi), \alpha\} \\ &= \sum_{i=1}^{j-1} \min\{w_i(\bar{\pi}), \alpha\} + \min\{c_j\beta_C, \alpha\} + \sum_{i=j+1}^k \min\{w_{i-1}(\bar{\pi}), \alpha\} \\ &= \sum_{i=1}^{k-1} \min\{w_i(\bar{\pi}), \alpha\} + \min\{c_j\beta_C, \alpha\}. \end{aligned}$$

As the proof of Proposition 1 and Proposition 2 does not depend on the value of k , it can be proved that

$$\begin{aligned} \sum_{i=1}^k \min\{w_i(\pi^*(\mathbf{s}^*)), \alpha\} &= \sum_{i=1}^{k-1} \min\{w_i(\bar{\pi}^*(\mathbf{s})), \alpha\} + \min\{c_j\beta_C, \alpha\} \\ &\leq \sum_{i=1}^{k-1} \min\{w_i(\bar{\mathbf{s}}, \bar{\pi}), \alpha\} + \min\{c_j\beta_C, \alpha\} \\ &= \sum_{i=1}^k \min\{w_i(\mathbf{s}, \pi), \alpha\} \end{aligned}$$

- When $j < p_{max}$, we will finish the proof in two parts corresponding to Proposition 1 and Proposition 2, respectively.

Part 1: For arbitrary given \mathbf{s} as Proposition 1 shows, we have

$$\begin{aligned} MC(\mathbf{s}, \pi) &= \sum_{i=1}^k \min\{w_i(\pi), \alpha\} \\ &= \sum_{i=1}^{j-1} \min\{w_i(\bar{\pi}), \alpha\} + \min\{c_j\beta_C, \alpha\} \\ &\quad + \sum_{i=j+1}^p \min\{w_{i-1}(\bar{\pi}) - \beta_C, \alpha\} + \sum_{i=p+1}^k \min\{w_{i-1}(\bar{\pi}), \alpha\} \\ &= \sum_{i=1}^{j-1} \min\{w_i(\bar{\pi}), \alpha\} + \min\{c_j\beta_C, \alpha\} \\ &\quad + \sum_{i=j}^{p-1} \min\{w_i(\bar{\pi}) - \beta_C, \alpha\} + \sum_{i=p}^{k-1} \min\{w_i(\bar{\pi}), \alpha\}, \end{aligned}$$

where $w_i(\bar{\pi}) = a_i(\bar{\pi})\beta_I + b_i(\bar{\pi})\beta_C$. Let

$$w'_i(\bar{\pi}) = a'_i(\bar{\pi})\beta_I + b'_i(\bar{\pi})\beta_C = \begin{cases} w_i(\bar{\pi}), & \text{if } 1 \leq i \leq j-1 \\ w_i(\bar{\pi}) - \beta_C, & \text{if } j \leq i \leq p-1 \\ w_i(\bar{\pi}), & \text{if } p \leq i \leq k-1 \end{cases}$$

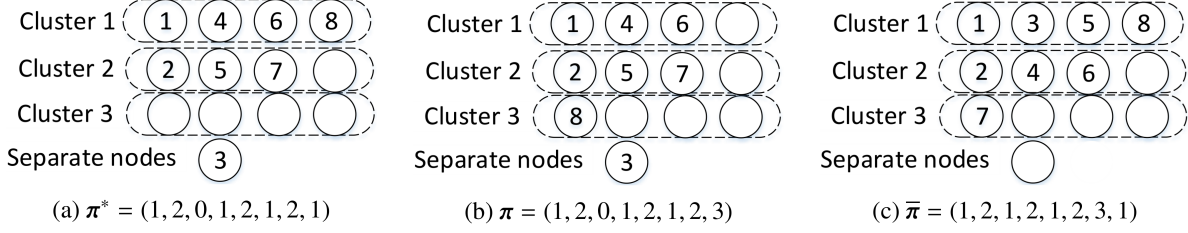


Fig. 12: Three cluster orders π^* , π and $\bar{\pi}$ for the CSN-DSS model.

then $a'_i(\bar{\pi}) = a_i(\bar{\pi})$ and

$$b'_i(\bar{\pi}) = \begin{cases} b_i(\bar{\pi}), & \text{if } 1 \leq i \leq j-1 \\ b_i(\bar{\pi}) - 1, & \text{if } j \leq i \leq p-1 \\ 0, & \text{if } p \leq i \leq k-1 \end{cases}$$

Although $b'_i(\bar{\pi}) = b_i(\bar{\pi}) - 1$ for $j \leq i \leq p-1$, the properties of the coefficient sequences will not change. Assume p^* is the value satisfying that

$$b_{p^*}(\pi^*) = 0, \text{ and } b_{p^*-1}(\pi^*) > 0.$$

When $1 \leq i \leq p^*$ and $j < p^*$,

$$\phi_i(\bar{\pi}^*) = \begin{cases} d - i + 1, & \text{if } 1 \leq i \leq j-1 \\ d - i, & \text{if } j \leq i \leq p^*. \end{cases} \quad (26)$$

and

$$\phi_i(\bar{\pi}) \geq \begin{cases} d - i + 1, & \text{if } 1 \leq i \leq j-1 \\ d - i, & \text{if } j \leq i \leq p^*. \end{cases} \quad (27)$$

With similar methods of Proposition 1, it can be proved that

$$\sum_{i=1}^{k-1} \min\{w'_i(\bar{\pi}^*), \alpha\} \leq \sum_{i=1}^{k-1} \min\{w'_i(\bar{\pi}), \alpha\}. \quad (28)$$

Hence, $MC(\mathbf{s}, \pi^*) \leq MC(\mathbf{s}, \pi)$.

Part 2: Next we will prove that $MC(\mathbf{s}^*, \pi^*(\mathbf{s}^*)) \leq MC(\mathbf{s}, \pi^*(\mathbf{s}))$ as proved in Proposition 2. With Algorithm 1, it's easy to verify that sequence $(w'_i(\bar{\pi}^*(\mathbf{s})), \dots, w'_{k-1}(\bar{\pi}^*(\mathbf{s})))$ is non-increasing. Although the values of $b'_i(\bar{\pi}^*(\mathbf{s}))$ may change when $i > j$, the relation between $w'_i(\bar{\pi}^*(\mathbf{s}))$ and $w'_i(\bar{\pi}^*(\mathbf{s}^*))$ won't be influenced. Similarly to the method used in Proposition 2, we can prove $w'_i(\bar{\pi}^*(\mathbf{s})) \geq w'_i(\bar{\pi}^*(\mathbf{s}^*))$ for $1 \leq i \leq k-1$. Hence,

$$MC(\mathbf{s}^*, \pi^*(\mathbf{s}^*)) \leq MC(\mathbf{s}, \pi^*(\mathbf{s})) \leq MC(\mathbf{s}, \pi).$$

APPENDIX B PROOF OF THEOREM 2

In this proof, we will compare MC_j^* and MC_{j+1}^* for $1 \leq j \leq k-1$. As $MC_j^* = \sum_{i=1}^k \min\{w_i(\pi^{(j)}), \alpha\}$, both $w_i(\pi^{(j)})$ and α need to be taken into consideration. Hence, this proof consists of two aspects. We first compare $[w_i(\pi^{(j)})]_{i=1}^k$ and $[w_i(\pi^{(j+1)})]_{i=1}^k$ one by one. Through analysing the cluster orders $\pi^{(j)}$ and $\pi^{(j+1)}$ (i.e., Figure 13), we enumerate all the possible cases of $[w_i(\pi^{(j)})]_{i=1}^k$ and $[w_i(\pi^{(j+1)})]_{i=1}^k$. Second, we calculate and compare MC_j^* and MC_{j+1}^* concretely in **Case**

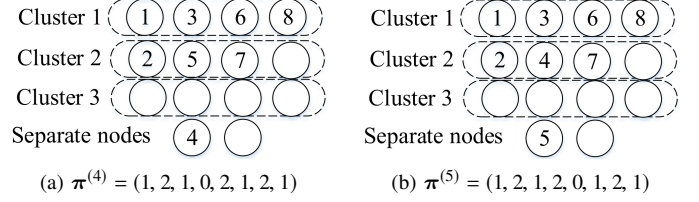


Fig. 13: The cluster orders $\pi^{(4)}$ and $\pi^{(5)}$ are corresponding to $\mathbf{s} = (1, 4, 3, 0)$, where the separate selected node locations are 4 and 5, respectively

1 and Case 2 by considering α . The details of this proof are as follows.

Through comparing $\pi^{(j)}$ and $\pi^{(j+1)}$, we can find

$$w_i(\pi^{(j)}) = w_i(\pi^{(j+1)}), \quad (29)$$

for $i \in [k] \setminus \{j, j+1\}$ ⁴. As Figure 13 shows, the first three and the last three selected nodes of $\pi^{(4)}$ and $\pi^{(5)}$ are at the same locations. Then we only need to compare

$$\begin{aligned} w_j(\pi^{(j)}) &= (d_I + d_C + 1 - j)\beta_C, \\ w_{j+1}(\pi^{(j)}) &= a_{j+1}(\pi^{(j)})\beta_I + b_{j+1}(\pi^{(j)})\beta_C \end{aligned}$$

and

$$\begin{aligned} w_j(\pi^{(j+1)}) &= a_j(\pi^{(j+1)})\beta_I + b_j(\pi^{(j+1)})\beta_C, \\ w_{j+1}(\pi^{(j+1)}) &= (d_I + d_C - j)\beta_C. \end{aligned}$$

Based on (8) and $\beta_I \geq \beta_C$,

$$\begin{aligned} w_{j+1}(\pi^{(j)}) &\geq a_{j+1}(\pi^{(j)})\beta_C + b_{j+1}(\pi^{(j)})\beta_C \\ &= (d_I + d_C - j)\beta_C \\ &= w_{j+1}(\pi^{(j+1)}), \\ w_j(\pi^{(j+1)}) &\geq a_j(\pi^{(j)})\beta_C + b_j(\pi^{(j)})\beta_C \\ &= (d_I + d_C + 1 - j)\beta_C \\ &= w_j(\pi^{(j)}). \end{aligned} \quad (30)$$

As proven in Lemma 1, $a_{j+1}(\pi^{(j)}) = d_I + 1 - h_{\pi^{(j)}}(j+1)$ and $a_j(\pi^{(j+1)}) = d_I + 1 - h_{\pi^{(j+1)}}(j)$. We can verify that the separate node will not influence the properties of a_i and b_i . Hence,

$$a_{j+1}(\pi^{(j)}) = a_j(\pi^{(j+1)}) \quad (32)$$

based on (2), the definition of $h_{\pi}(\cdot)$. In Figure 13, $a_5(\pi^{(4)}) = 2 = a_4(\pi^{(5)})$. Then

$$b_j(\pi^{(j+1)}) = b_{j+1}(\pi^{(j)}) + 1, \quad (33)$$

⁴[k] represents the integer set $\{1, 2, \dots, k\}$.

because of formula (8) in Lemma 2. Hence,

$$w_j(\boldsymbol{\pi}^{(j+1)}) - w_{j+1}(\boldsymbol{\pi}^{(j)}) = \beta_C > 0. \quad (34)$$

On the other hand, $w_j(\boldsymbol{\pi}^{(j)}) - w_{j+1}(\boldsymbol{\pi}^{(j+1)}) = \beta_C$. Thus

$$w_j(\boldsymbol{\pi}^{(j+1)}) + w_{j+1}(\boldsymbol{\pi}^{(j+1)}) = w_j(\boldsymbol{\pi}^{(j)}) + w_{j+1}(\boldsymbol{\pi}^{(j)}) \quad (35)$$

With (30) (31) and (34), we can find that $w_j(\boldsymbol{\pi}^{(j+1)})$ is the largest and $w_{j+1}(\boldsymbol{\pi}^{(j+1)})$ is the smallest among $w_j(\boldsymbol{\pi}^{(j)})$, $w_{j+1}(\boldsymbol{\pi}^{(j)})$, $w_j(\boldsymbol{\pi}^{(j+1)})$ and $w_{j+1}(\boldsymbol{\pi}^{(j+1)})$. Hence, we only need to analyse the following two cases and consider α .

Case 1: $w_j(\boldsymbol{\pi}^{(j+1)}) \geq w_j(\boldsymbol{\pi}^{(j)}) \geq w_{j+1}(\boldsymbol{\pi}^{(j)}) \geq w_{j+1}(\boldsymbol{\pi}^{(j+1)})$.

1) When $\alpha \geq w_j(\boldsymbol{\pi}^{(j+1)})$, based on (35),

$$\begin{aligned} & \min \{w_j(\boldsymbol{\pi}^{(j+1)}), \alpha\} + \min \{w_{j+1}(\boldsymbol{\pi}^{(j+1)}), \alpha\} \\ &= w_j(\boldsymbol{\pi}^{(j+1)}) + w_{j+1}(\boldsymbol{\pi}^{(j+1)}) \\ &= w_j(\boldsymbol{\pi}^{(j)}) + w_{j+1}(\boldsymbol{\pi}^{(j)}) \\ &= \min \{w_j(\boldsymbol{\pi}^{(j)}), \alpha\} + \min \{w_{j+1}(\boldsymbol{\pi}^{(j)}), \alpha\}. \end{aligned}$$

Hence, $MC_j^* = MC_{j+1}^*$.

2) When $w_j(\boldsymbol{\pi}^{(j+1)}) \geq \alpha \geq w_j(\boldsymbol{\pi}^{(j)})$,

$$\begin{aligned} & \min \{w_j(\boldsymbol{\pi}^{(j+1)}), \alpha\} + \min \{w_{j+1}(\boldsymbol{\pi}^{(j+1)}), \alpha\} \\ & \leq w_j(\boldsymbol{\pi}^{(j+1)}) + w_{j+1}(\boldsymbol{\pi}^{(j+1)}) \\ & \stackrel{(a)}{=} w_j(\boldsymbol{\pi}^{(j)}) + w_{j+1}(\boldsymbol{\pi}^{(j)}) \\ & \stackrel{(b)}{=} \min \{w_j(\boldsymbol{\pi}^{(j)}), \alpha\} + \min \{w_{j+1}(\boldsymbol{\pi}^{(j)}), \alpha\}, \end{aligned}$$

where (a) results from (35) and (b) is based on $\alpha \geq w_j(\boldsymbol{\pi}^{(j)}) \geq w_{j+1}(\boldsymbol{\pi}^{(j)})$. Hence,

$$MC_j^* \geq MC_{j+1}^*.$$

3) When $w_j(\boldsymbol{\pi}^{(j)}) \geq \alpha \geq w_{j+1}(\boldsymbol{\pi}^{(j)})$,

$$\begin{aligned} & \min \{w_j(\boldsymbol{\pi}^{(j+1)}), \alpha\} + \min \{w_{j+1}(\boldsymbol{\pi}^{(j+1)}), \alpha\} \\ &= \alpha + w_{j+1}(\boldsymbol{\pi}^{(j+1)}) \\ & \stackrel{(a)}{\leq} \alpha + w_{j+1}(\boldsymbol{\pi}^{(j)}) \\ & \stackrel{(b)}{=} \min \{w_j(\boldsymbol{\pi}^{(j)}), \alpha\} + \min \{w_{j+1}(\boldsymbol{\pi}^{(j)}), \alpha\}, \end{aligned}$$

where (a) and (b) are based on $w_{j+1}(\boldsymbol{\pi}^{(j+1)}) \leq w_{j+1}(\boldsymbol{\pi}^{(j)}) \leq \alpha \leq w_j(\boldsymbol{\pi}^{(j)})$. Hence,

$$MC_j^* \geq MC_{j+1}^*.$$

4) When $w_{j+1}(\boldsymbol{\pi}^{(j)}) \geq \alpha \geq w_{j+1}(\boldsymbol{\pi}^{(j+1)})$,

$$\begin{aligned} & \min \{w_j(\boldsymbol{\pi}^{(j+1)}), \alpha\} + \min \{w_{j+1}(\boldsymbol{\pi}^{(j+1)}), \alpha\} \\ &= \alpha + w_{j+1}(\boldsymbol{\pi}^{(j+1)}) \\ & \stackrel{(a)}{\leq} \alpha + \alpha \\ & \stackrel{(b)}{=} \min \{w_j(\boldsymbol{\pi}^{(j)}), \alpha\} + \min \{w_{j+1}(\boldsymbol{\pi}^{(j)}), \alpha\}, \end{aligned}$$

where (a) and (b) are based on $w_{j+1}(\boldsymbol{\pi}^{(j+1)}) \leq \alpha \leq w_{j+1}(\boldsymbol{\pi}^{(j)}) \leq w_j(\boldsymbol{\pi}^{(j)})$. Hence,

$$MC_j^* \geq MC_{j+1}^*.$$

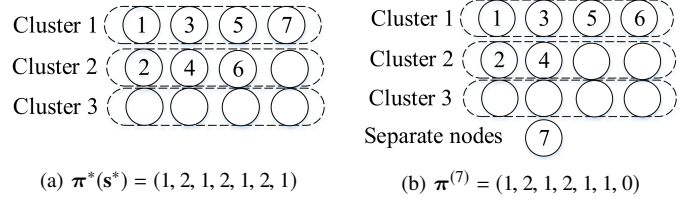


Fig. 14: In (a), the cluster order is $\boldsymbol{\pi}^*(\mathbf{s}^*)$ for $\mathbf{s}^* = (0, 4, 3, 0)$, which achieves the capacity of the cluster DSS model. In (b), the cluster order and selected node distribution are $\boldsymbol{\pi}^{(7)}$ and $\mathbf{s}^* = (1, 4, 2, 0)$ respectively, achieving the capacity of the CSN-DSS model.

5) When $w_{j+1}(\boldsymbol{\pi}^{(j+1)}) \geq \alpha$,

$$\begin{aligned} & \min \{w_j(\boldsymbol{\pi}^{(j+1)}), \alpha\} + \min \{w_{j+1}(\boldsymbol{\pi}^{(j+1)}), \alpha\} \\ &= \alpha + \alpha \\ &= \min \{w_j(\boldsymbol{\pi}^{(j)}), \alpha\} + \min \{w_{j+1}(\boldsymbol{\pi}^{(j)}), \alpha\}, \end{aligned}$$

and $MC_j^* = MC_{j+1}^*$.

Case 2: $w_j(\boldsymbol{\pi}^{(j+1)}) \geq w_{j+1}(\boldsymbol{\pi}^{(j)}) \geq w_j(\boldsymbol{\pi}^{(j)}) \geq w_{j+1}(\boldsymbol{\pi}^{(j+1)})$. When $\alpha \geq w_j(\boldsymbol{\pi}^{(j+1)})$, $w_j(\boldsymbol{\pi}^{(j+1)}) \geq \alpha \geq w_{j+1}(\boldsymbol{\pi}^{(j)})$, $w_j(\boldsymbol{\pi}^{(j)}) \geq \alpha \geq w_{j+1}(\boldsymbol{\pi}^{(j+1)})$ and $w_{j+1}(\boldsymbol{\pi}^{(j+1)}) \geq \alpha$, the situations are similar to Case 1: 1, 2, 4, 5, respectively, and can be analysed with the same methods. We only need to consider the situation that $w_{j+1}(\boldsymbol{\pi}^{(j)}) \geq \alpha \geq w_j(\boldsymbol{\pi}^{(j)}) \geq w_{j+1}(\boldsymbol{\pi}^{(j+1)})$. Then

$$\begin{aligned} & \min \{w_j(\boldsymbol{\pi}^{(j+1)}), \alpha\} + \min \{w_{j+1}(\boldsymbol{\pi}^{(j+1)}), \alpha\} \\ &= \alpha + w_{j+1}(\boldsymbol{\pi}^{(j+1)}) \\ & \leq \alpha + w_j(\boldsymbol{\pi}^{(j)}) \\ &= \min \{w_{j+1}(\boldsymbol{\pi}^{(j)}), \alpha\} + \min \{w_j(\boldsymbol{\pi}^{(j)}), \alpha\}. \end{aligned}$$

Hence, $MC_j^* \geq MC_{j+1}^*$ and we finish the proof.

APPENDIX C PROOF OF THEOREM 4

In this proof, we need to compare the capacities of the cluster DSS and the system after adding a separate node, which are represented by $\boldsymbol{\pi}^*(\mathbf{s}^*)$ and $\boldsymbol{\pi}^{(k)}$ respectively, as shown in Proposition 2 and Theorem 3. By analysing cluster orders $\boldsymbol{\pi}^*(\mathbf{s}^*)$ and $\boldsymbol{\pi}^{(k)}$, we compare the part incoming weights $[w_i(\boldsymbol{\pi}^*(\mathbf{s}^*))]_{i=1}^k$ and $[w_i(\boldsymbol{\pi}^{(k)})]_{i=1}^k$ one by one and enumerate all possible cases. We finish the proof in two parts. Part one investigates the case $R \mid k$, where adding a separate node will not change the capacity corresponding to Example 2. In the second part, we consider the case $R \nmid k$, where the system capacity is reduced (see Example 1).

Part 1 ($R \mid k$): As illustrated in Figure 11, the components of cluster order $\boldsymbol{\pi}^*(\mathbf{s}^*)$ and $\boldsymbol{\pi}^{(k)}$ are the same except the k -th one. Hence, the part incoming weight (defined in Subsection II-D) satisfies that

$$w_i(\boldsymbol{\pi}^*(\mathbf{s}^*)) = w_i(\boldsymbol{\pi}^{(k)}),$$

for $1 \leq i \leq k-1$. We only need to compare $w_k(\boldsymbol{\pi}^*(\mathbf{s}^*))$ and $w_k(\boldsymbol{\pi}^{(k)})$. When $R \mid k$, based on the horizontal selection algorithm, we can verify that $h_{\boldsymbol{\pi}^*(\mathbf{s}^*)}(k) = R$. Because of

Lemma 1 and Lemma 2, $a_k(\pi^*(\mathbf{s}^*)) = d_I + 1 - h_{\pi^*(\mathbf{s}^*)}(k) = 0$ and $b_k(\pi^*(\mathbf{s}^*)) = d_I + d_C + 1 - k - a_k(\pi^*(\mathbf{s}^*)) = R - k + d_C$. On the other hand, $w_k(\pi^{(k)}) = (d_I + d_C + 1 - k)\beta_C = (R - k + d_C)\beta_C$ because of formula (3). Hence, $w_k(\pi^*(\mathbf{s}^*)) = 0\beta_I + (R - k + d_C)\beta_C = w_k(\pi^{(k)})$. Therefore, adding one separate node will not change the system capacity.

Part 2 ($R \nmid k$): When $R \nmid k$, there are two cases: $k < R$ and $k \geq R$.

- **Case 1** ($k < R$): In this case, all the selected nodes in $\pi^*(\mathbf{s}^*)$ are in Cluster 1. For $\pi^{(k)}$, the first $k - 1$ selected nodes are also in cluster 1. Hence, $w_i(\pi^*(\mathbf{s}^*)) = w_i(\pi^{(k)})$ for $1 \leq i \leq k - 1$ and

$$\begin{aligned} w_k(\pi^*(\mathbf{s}^*)) &= a_k(\pi^*(\mathbf{s}^*))\beta_I + d_C\beta_C \\ &\stackrel{(a)}{=} (d_I + d_C + 1 - k - d_C)\beta_I + d_C\beta_C \\ &= (R - k)\beta_I + d_C\beta_C, \\ w_k(\pi^{(k)}) &= (d_I + d_C + 1 - k)\beta_C = (R - k + d_C)\beta_C, \end{aligned}$$

where (a) is because of Lemma 2. Hence, $w_k(\pi^*(\mathbf{s}^*)) - w_k(\pi^{(k)}) = (R - k)(\beta_I - \beta_C) \geq 0$ and $\sum_{i=1}^k \min\{w_i(\pi^*(\mathbf{s}^*)), \alpha\} \geq \sum_{i=1}^k \min\{w_i(\pi^{(k)}), \alpha\}$, indicating that adding one separate node reduces the system capacity.

- **Case 2** ($k \geq R$): As $R \nmid k$, let

$$q \triangleq \lfloor k/R \rfloor, \quad (36)$$

$$r \triangleq k \pmod R. \quad (37)$$

Obviously, $1 \leq q \leq L - 1$ and $1 \leq r \leq k - 1$. All nodes in the first q clusters and r nodes in the $(q + 1)$ -th cluster are selected nodes based on the horizontal selection algorithm. Comparing each components of $\pi^*(\mathbf{s}^*)$ and $\pi^{(k)}$, we can find that

$$w_i(\pi^*(\mathbf{s}^*)) = w_i(\pi^{(k)}) \quad (38)$$

for $1 \leq i \leq (q + 1)r - 1$.

In cluster order $\pi^{(k)}$, the first $k - 1$ selected nodes are cluster nodes, and there are $r - 1$ selected nodes in the $(q - 1)$ -th cluster. As mentioned in Subsection II-D, the nodes in cluster orders are numbered and grouped column by column. For cluster order $\pi^{(k)}$, there are $q + 1$ selected nodes in each of the first r columns and q selected nodes in each of the remaining $R - r$ columns. When a separate selected node is added, some of the numbers of selected cluster nodes will change. There are $q + 1$ selected nodes in each of the first $r - 1$ columns and q selected nodes in the remaining $R - r + 1$ columns in $\pi^{(k)}$. As the selected cluster node are numbered from left to right column by column, the numbers of the first $(q + 1)r - 1$ selected nodes will not change, leading to equation (38). An example is illustrated as follows.

In Figure 14, the selected nodes are numbered by cluster orders $\pi^*(\mathbf{s}^*)$ and $\pi^{(7)}$ in (a) and (b), respectively, where $R = 4$, $k = 7$, $q = \lfloor k/R \rfloor = 1$ and $r = 3$. In Figure 14 (a), there are $q + 1 = 2$ selected nodes in each of the first $r = 3$ column and 1 selected nodes in the last one columns. In Figure 14 (b), there are $q + 1 = 2$ selected nodes in each of the first $r - 1 = 2$ columns and $q = 1$ selected nodes in each of the remaining $R - r + 1 = 2$ columns. We can verify

that the locations of the first $(q + 1)r - 1 = 2 \times 3 - 1 = 5$ selected nodes, namely node 1 to node 5, will not change. However, the locations of other nodes have changed. For example, node 6 is the third selected node in cluster 2 in $\pi^*(\mathbf{s}^*)$, but the 6th node in $\pi^{(7)}$ is the 4th one in cluster 1, leading to the difference of $w_6(\pi^*(\mathbf{s}^*))$ and $w_6(\pi^{(7)})$. When $i = (q + 1)r$, as shown in Figure 14, the i -th node in $\pi^*(\mathbf{s}^*)$ is in a different column than that in $\pi^{(k)}$ and $h_{\pi^{(k)}}(i) = h_{\pi^*(\mathbf{s}^*)}(i) + 1$. Hence, $a_i(\pi^*(\mathbf{s}^*)) = d_I + 1 - h_{\pi^*(\mathbf{s}^*)}(i) = d_I + 1 - h_{\pi^{(k)}}(i) + 1 = a_i(\pi^{(k)}) + 1$. Based on Lemma 2, $a_i(\pi^*(\mathbf{s}^*)) + b_i(\pi^*(\mathbf{s}^*)) = a_i(\pi^{(k)}) + b_i(\pi^{(k)})$, then

$$b_i(\pi^*(\mathbf{s}^*)) = b_i(\pi^{(k)}) - 1.$$

Hence, $w_i(\pi^*(\mathbf{s}^*)) - w_i(\pi^{(k)}) = \beta_I - \beta_C \geq 0$.

For example, in Figure 14, $w_6(\pi^*(\mathbf{s}^*)) = (d_I - 2)\beta_I + (d_C - 3)\beta_C = \beta_I + (d_C - 3)\beta_C$ and $w_6(\pi^{(k)}) = (d_I - 3)\beta_I + (d_C - 2)\beta_C = (d_C - 2)\beta_C$. Hence, $w_6(\pi^*(\mathbf{s}^*)) - w_6(\pi^{(k)}) = \beta_I - \beta_C$.

When $(q + 1)r < i \leq k - 1$, there are only two possible cases about the relationship of node i in $\pi^*(\mathbf{s}^*)$ and $\pi^{(k)}$.

- **Subcase 1:** The column number of node i in $\pi^*(\mathbf{s}^*)$ equals that in $\pi^{(k)}$, namely, $h_{\pi^*(\mathbf{s}^*)}(i) = h_{\pi^{(k)}}(i)$. For example, in Figure 9, the 4th nodes in $\pi^*(\mathbf{s}^*)$ and $\pi^{(9)}$ are both in the second column. So $h_{\pi^*(\mathbf{s}^*)}(4) = h_{\pi^{(9)}}(4) = 2$. Similarly, $h_{\pi^*(\mathbf{s}^*)}(6) = h_{\pi^{(9)}}(6) = 3$ and $h_{\pi^*(\mathbf{s}^*)}(8) = h_{\pi^{(9)}}(8) = 4$.

Based on Lemma 1 and Lemma 2, we can get

$$a_i(\pi^*(\mathbf{s}^*)) = a_i(\pi^{(k)}) \text{ and } b_i(\pi^*(\mathbf{s}^*)) = b_i(\pi^{(k)}).$$

Therefore, $w_i(\pi^*(\mathbf{s}^*)) = w_i(\pi^{(k)})$.

- **Subcase 2:** The column number of node i in $\pi^*(\mathbf{s}^*)$ is smaller than that in $\pi^{(k)}$ by 1, namely, $h_{\pi^*(\mathbf{s}^*)}(i) = h_{\pi^{(k)}}(i) - 1$. In Figure 9, the 5th node in $\pi^*(\mathbf{s}^*)$ is in the second column, while the 5th node in $\pi^{(9)}$ is in the third column. Hence, $h_{\pi^*(\mathbf{s}^*)}(5) = 2 = h_{\pi^{(9)}}(5) - 1$. Similarly, $h_{\pi^*(\mathbf{s}^*)}(7) = 3 = h_{\pi^{(9)}}(7) - 1$.

Based on Lemma 1 and Lemma 2,

$$a_i(\pi^*(\mathbf{s}^*)) = a_i(\pi^{(k)}) + 1 \text{ and } b_i(\pi^*(\mathbf{s}^*)) = b_i(\pi^{(k)}) - 1,$$

Hence, $w_i(\pi^*(\mathbf{s}^*)) - w_i(\pi^{(k)}) = \beta_I - \beta_C \geq 0$

Combining the above 2 subcases, it is proved that $w_i(\pi^*(\mathbf{s}^*)) \geq w_i(\pi^{(k)})$ for $(q + 1)r < i \leq k - 1$. When $i = k$, based on Algorithm 1 and 2, the k -th selected node in $\pi^*(\mathbf{s}^*)$ is the R -th one in its cluster, namely, $h_{\pi^*(\mathbf{s}^*)}(k) = R$. Based on Lemma 1 and Lemma 2, $a_k(\pi^*(\mathbf{s}^*)) = d_I + 1 - h_{\pi^*(\mathbf{s}^*)}(k) = 0$ and $w_k(\pi^*(\mathbf{s}^*)) = a_k(\pi^*(\mathbf{s}^*))\beta_I + (d_I + d_C + 1 - k - a_k(\pi^*(\mathbf{s}^*)))\beta_C = (d_C + R - k)\beta_C$. As $w_k(\pi^{(k)}) = (d_I + d_C + 1 - k)\beta_C = (d_C + R - k)\beta_C$, then $w_k(\pi^*(\mathbf{s}^*)) = w_k(\pi^{(k)})$.

Hence, when $R \nmid k$, $w_i(\pi^*(\mathbf{s}^*)) \geq w_i(\pi^{(k)})$ for $1 \leq i \leq k$. Then $MC(\mathbf{s}^*, \pi^*(\mathbf{s}^*)) \geq MC(\pi^{(k)})$. We finish the proof.

ACKNOWLEDGMENT

This work was partially supported by China Program of International S&T Cooperation 2016YFE0100300, the National Natural Science Foundation of China under Grant 61571293 and SJTU-CUHK Joint Research Collaboration Fund 2018.

REFERENCES

- [1] V. Abdrashitov, N. Prakash, and M. Médard. The storage vs repair bandwidth trade-off for multiple failures in clustered storage networks. In *2017 IEEE Information Theory Workshop (ITW)*, pages 46–50, Nov 2017.
- [2] V. Aggarwal, Y. R. Chen, T. Lan, and Y. Xiang. Sprout: A functional caching approach to minimize service latency in erasure-coded storage. *IEEE/ACM Transactions on Networking*, 25(6):3683–3694, Dec 2017.
- [3] R. Ahlswede, N. Cai, S. Y. R. Li, and R. W. Yeung. Network information flow. *IEEE Trans. Inf. Theor.*, 46(4):1204–1216, September 2006.
- [4] F. Ahmad, S. T. Chakradhar, A. Raghunathan, and T. N. Vijaykumar. Shufflewatcher: Shuffle-aware scheduling in multi-tenant mapreduce clusters. In *2014 USENIX Annual Technical Conference (USENIX ATC 14)*, pages 1–13, Philadelphia, PA, 2014. USENIX Association.
- [5] R. K. Ahuja, T. L. Magnanti, and J. B. Orlin. *Network Flows: Theory, Algorithms, and Applications*. Prentice Hall, 1 edition, 1993.
- [6] S. Akhlaghi, A. Kiani, and M. R. Ghanavati. Cost-bandwidth tradeoff in distributed storage systems. *Computer Communications*, 33(17):2105 – 2115, 2010. Special Issue: Applied sciences in communication technologies.
- [7] A. O. Al-Abbasi and V. Aggarwal. Video streaming in distributed erasure-coded storage systems: Stall duration analysis. *IEEE/ACM Transactions on Networking*, 26(4):1921–1932, Aug 2018.
- [8] T. Benson, A. Akella, and D. A. Maltz. Network traffic characteristics of data centers in the wild. In *Proceedings of the 10th ACM SIGCOMM Conference on Internet Measurement, IMC '10*, pages 267–280, New York, NY, USA, 2010. ACM.
- [9] A. G. Dimakis, P. B. Godfrey, Y. Wu, M. J. Wainwright, and K. Ramchandran. Network coding for distributed storage systems. *IEEE Trans. Inf. Theory*, 56(9):4539–4551, Sept 2010.
- [10] A. G. Dimakis, K. Ramchandran, Y. Wu, and C. Suh. A survey on network codes for distributed storage. *Proceedings of the IEEE*, 99(3):476–489, March 2011.
- [11] T. Ernvall, S. El Rouayheb, C. Hollanti, and H. V. Poor. Capacity and security of heterogeneous distributed storage systems. *IEEE Journal on Selected Areas in Communications*, 31(12):2701–2709, December 2013.
- [12] D. Ford, F. Labelle, F. I Popovici, M. Stokely, V. Truong, L. Barroso, C. Grimes, and S. Quinlan. Availability in globally distributed storage systems. In *OsdI*, volume 10, pages 1–7, 2010.
- [13] S. Goparaju, A. Fazeli, and A. Vardy. Minimum storage regenerating codes for all parameters. *IEEE Trans. Inf. Theory*, 63(10):6318–6328, Oct 2017.
- [14] H. Hou, P. P. C. Lee, K. W. Shum, and Y. Hu. Rack-aware regenerating codes for data centers. *CoRR*, abs/1802.04031, 2018.
- [15] Y. Hu, P. P. C. Lee, and X. Zhang. Double regenerating codes for hierarchical data centers. In *2016 IEEE International Symposium on Information Theory (ISIT)*, pages 245–249, July 2016.
- [16] Y. Hu, X. Li, M. Zhang, P. P. C. Lee, X. Zhang, P. Zhou, and D. Feng. Optimal repair layering for erasure-coded data centers: From theory to practice. *ACM Trans. Storage*, 13(4):33:1–33:24, November 2017.
- [17] C. Huang, M. Chen, and J. Li. Pyramid codes: Flexible schemes to trade space for access efficiency in reliable data storage systems. *Trans. Storage*, 9(1):3:1–3:28, March 2013.
- [18] J. Kubiawicz, D. Bindel, Y. Chen, S. Czerwinski, P. Eaton, D. Geels, R. Gummedi, S. Rhea, H. Weatherspoon, W. Weimer, C. Wells, and B. Zhao. Oceanstore: An architecture for global-scale persistent storage. *SIGPLAN Not.*, 35(11):190–201, November 2000.
- [19] J. Li and B. Li. Beehive: Erasure codes for fixing multiple failures in distributed storage systems. *IEEE Transactions on Parallel and Distributed Systems*, 28(5):1257–1270, May 2017.
- [20] J. Li, S. Yang, X. Wang, and B. Li. Tree-structured data regeneration in distributed storage systems with regenerating codes. In *2010 Proceedings IEEE INFOCOM*, pages 1–9, March 2010.
- [21] S. Y. R. Li, R. W. Yeung, and N. Cai. Linear network coding. *IEEE Trans. Inf. Theory*, 49(2):371–381, February 2003.
- [22] J. Pernas, C. Yuen, B. Gastón, and J. Pujol. Non-homogeneous two-rack model for distributed storage systems. In *2013 IEEE International Symposium on Information Theory*, pages 1237–1241, July 2013.
- [23] N. Prakash, V. Abdrashitov, and M. Médard. The storage vs repair-bandwidth trade-off for clustered storage systems. *CoRR*, abs/1701.04909, 2017.
- [24] K. V. Rashmi, N. B. Shah, and P. V. Kumar. Optimal exact-regenerating codes for distributed storage at the msr and mbr points via a product-matrix construction. *IEEE Trans. Inf. Theory*, 57(8):5227–5239, Aug 2011.
- [25] B. Shao, D. Song, G. Bian, and Y. Zhao. Rack aware data placement for network consumption in erasure-coded clustered storage systems. *Information*, 9(7), 2018.
- [26] M. Sipos, J. Gahm, N. Venkat, and D. Oran. Network-aware feasible repairs for erasure-coded storage. *IEEE/ACM Transactions on Networking*, 26(3):1404–1417, June 2018.
- [27] J. Sohn, B. Choi, S. W. Yoon, and J. Moon. Capacity of clustered distributed storage. In *2017 IEEE International Conference on Communications (ICC)*, May 2017.
- [28] J. Sohn, B. Choi, S. W. Yoon, and J. Moon. Capacity of clustered distributed storage. *IEEE Transactions on Information Theory*, 65(1):81–107, Jan 2019.
- [29] X. Tang, B. Yang, J. Li, and H. D. L. Hollmann. A new repair strategy for the hadamard minimum storage regenerating codes for distributed storage systems. *IEEE Transactions on Information Theory*, 61(10):5271–5279, Oct 2015.
- [30] A. Vahdat, M. Al-Fares, N. Farrington, R. N. Mysore, G. Porter, and S. Radhakrishnan. Scale-out networking in the data center. *IEEE Micro*, 30(4):29–41, July 2010.
- [31] J. Wang, T. Wang, and Y. Luo. Storage and repair bandwidth tradeoff for distributed storage systems with clusters and separate nodes. *Science China Information Sciences*, 61(10):100303, Aug 2018.
- [32] Y. Wang, D. Wei, X. Yin, and X. Wang. Heterogeneity-aware data regeneration in distributed storage systems. In *IEEE INFOCOM 2014 - IEEE Conference on Computer Communications*, pages 1878–1886, April 2014.
- [33] Y. Wu and A. G. Dimakis. Reducing repair traffic for erasure coding-based storage via interference alignment. In *Information Theory, 2009. ISIT 2009. IEEE International Symposium on*, pages 2276–2280. IEEE, 2009.
- [34] Y. Xiang, T. Lan, V. Aggarwal, and Y. R. Chen. Joint latency and cost optimization for erasure-coded data center storage. *IEEE/ACM Transactions on Networking*, 24(4):2443–2457, Aug 2016.
- [35] B. Yang, X. Tang, and J. Li. A systematic piggybacking design for minimum storage regenerating codes. *IEEE Transactions on Information Theory*, 61(11):5779–5786, Nov 2015.
- [36] Q. Yu, K. W. Shum, and C. W. Sung. Tradeoff between storage cost and repair cost in heterogeneous distributed storage systems. *Transactions on Emerging Telecommunications Technologies*, 26(10):1201–1211, 2015.
- [37] H. Zhang, H. Li, and S. Y. R. Li. Repair tree: Fast repair for single failure in erasure-coded distributed storage systems. *IEEE Transactions on Parallel and Distributed Systems*, 28(6):1728–1739, June 2017.